1250

TRANSPORTATION RESEARCH RECORD

Innovation in Aggregate Testing

TRANSPORTATION RESEARCH BOARD
NATIONAL RESEARCH COUNCIL
WASHINGTON, D.C. 1989

Transportation Research Record 1250
Price: $7.50

mode
1 highway transportation

subject area
35 mineral aggregates

Printed in the United States of America

Library of Congress Cataloging-in-Publication Data
National Research Council. Transportation Research Board.

Innovation in aggregate testing.
p. cm.—(Transportation research record, ISSN 0361-1981 ; 1250)
Reports prepared for the 68th Annual Meeting of the Transportation Research Board.
ISBN 0-309-04969-5
1. Aggregates (Building materials)—Testing. 2. Concrete—Testing. I. National Research Council (U.S.). Transportation Research Board. Meeting (68th : 1987 : Washington, D.C.) II. Series.
TE7.H5 no. 1250
[TA441]
388 s—dc20
[620.1'91] 90-35107
CIP

Sponsorship of Transportation Research Record 1250

GROUP 2—DESIGN AND CONSTRUCTION OF TRANSPORTATION FACILITIES
Chairman: Raymond A. Forsyth, California Department of Transportation

Evaluations, Systems, and Procedures Section
Chairman: Terry M. Mitchell, Federal Highway Administration, U.S. Department of Transportation

Committee on Mineral Aggregates
Chairman: Vernon J. Marks, Iowa Department of Transportation
Bernard D. Alkire, David A. Anderson, Gordon W. Beecroft, Robert J. Collins, Warren B. Diederich, James R. Dunn, Stephen W. Forster, James G. Gehler, Robert F. Hinshaw, Richard C. Ingberg, George J. Kassal, Dah-Yinn Lee, Peter Malphurs, Charles R. Marek, Michael P. McCormick, Richard C. Meininger, John T. Paxton, Richard W. Petrarca, Barbara J. Smith, Kenneth R. Wardlaw, Lennard J. Wylde, John S. Youtcheff

G. P. Jayaprakash, Transportation Research Board staff

The organizational units, officers, and members are as of December 31, 1988.

Transportation Research Board publications are available by ordering directly from TRB. They may also be obtained on a regular basis through organizational or individual affiliation with TRB; affiliates or library subscribers are eligible for substantial discounts. For further information, write to the Transportation Research Board, National Research Council, 2101 Constitution Avenue, N.W., Washington, D.C. 20418.

Transportation Research Record 1250

Contents

Foreword

Aggregates make up 95 percent of all construction materials. The United States uses more than 8,000 pounds of aggregate per person per year. Durability of highway pavements and structures is highly dependent on the quality of aggregate used. Improved laboratory tests are needed to ensure that proper quality aggregates are used. The five papers included in this Record deal with new tests or evaluation of aggregates for specific applications. The papers are of interest to those who are concerned with quality or testing of construction aggregates.

Wang reports on evaluation of aggregate used in arrester beds to provide deceleration of runaway trucks. Testing of aggregate for use in arrester beds includes determination of gradation, interparticle friction, angularity, sphericity, and durability.

Crumpton, Smith, and Jayaprakash report on the use of portland cement concrete cups made from drilled cores to evaluate the deterioration due to sodium chloride salt. They indicate that the salt, without the action of freezing and thawing, can enhance deterioration of carbonate aggregate and the cement paste.

The use of X-ray diffraction and X-ray fluorescence to determine the quality of aggregate for portland cement concrete is presented by Dubberke and Marks. They used the shift in the maximum intensity X-ray diffraction d-spacing peak of dolomite to predict the performance of carbonate aggregates in portland cement concrete.

Meier and Elnicky studied the shape and surface texture of fine aggregate and their effect on stability of hot mix asphalt concrete. According to them, the best evaluation of fine aggregate shape and texture is obtained from the National Stone Association Test, the Rex and Peck time index, and specific rugosity by packing volume.

Graves, Eades, and Smith relate treatment of silica-carbonate materials with hydrated lime. This treatment done prior to testing, enhanced strength development by providing a readily available source of calcium carbonate cement. In addition, the treatment allowed for a rapid test method to determine the potential strength of silica-carbonate materials.

Aggregate Testing for Construction of Arrester Beds

M. C. WANG

This paper presents methods of testing aggregate for use in arrester beds. Also presented are test results of five aggregates and the performance of the aggregates in the arrester beds. The test aggregates were obtained from five existing arrester beds throughout Pennsylvania. They were Pennsylvania State University (PSU) river pea gravel, PSU crushed aggregate, Pleasant Gap gravel, Green Tree gravel, and Freeport gravel. Tests performed in the laboratory included gradation, specific gravity, Los Angeles abrasion, and freeze-thaw. In addition, particle angularity, sphericity, and shearing resistance were determined. The field performance of the test aggregates except Green Tree gravel was evaluated in terms of mean average truck deceleration in the bed. The available data show that PSU crushed aggregate performs most poorly of the four. The other three perform nearly equally well, although Pleasant Gap gravel has a static internal friction angle considerably lower than PSU river pea gravel. These results indicate that aggregate performance depends not only on interparticle friction but also on other properties such as particle angularity and sphericity. For long-term performance, particle durability is also an important factor. Thus, testing of aggregate for use in the arrester bed should involve determination of gradation, interparticle friction, angularity, sphericity, and durability.

When heavy vehicles such as trucks or tractor-trailers travel on highways with long, steep downgrades and lose their braking capabilities, property damage and loss of life often occur if they hit other vehicles, nearby buildings, or pedestrians. To save life and avoid property damage, there must be facilities along the highway that can stop runaway vehicles that are driven into them. Such facilities are often called escape ramps or arrester beds.

There are three main types of arrester beds: gravity ramp, sand piles, and gravel beds. Of these three types, gravel beds have been shown to be safer and more efficient.The field performance of gravel arrester beds depends greatly on two aggregate properties, namely interparticle friction and free drainage. The ideal condition is an interparticle friction low enough for tires to sink into the aggregate yet sufficiently high to stop the vehicle within a desired distance. This condition must be maintained throughout the entire service life of the arrester bed without being influenced by freezing and other possible adverse factors. The effect of freezing can be minimized by preventing the accumulation of excess water in the arrester bed. Therefore, the aggregate must be free-draining.

To possess both low interparticle friction and high permeability, the aggregate must have rounded particles with uniform gradation. A natural aggregate that can satisfy this requirement is pea gravel; for this reason, pea gravel has been used most often in the construction of arrester beds.

Department of Civil Engineering, The Pennsylvania State University, University Park, Pa. 16802

Although particle size and distribution are important factors influencing interparticle friction and drainage, other factors such as particle shape and surface texture are of equal importance. To maintain the original as-constructed level of performance, furthermore, the aggregate particles must be tough and durable. Thus, selection of aggregate for construction of arrester beds requires extensive testing to determine not only the grain size distribution but also other properties, including at least particle shape, angularity, durability, and shearing resistance. This paper presents test methods, test results for five different aggregates, and the relation between the measured aggregate properties and field performance.

TEST AGGREGATES

The aggregates tested were obtained from escape ramps located at the Pennsylvania State University (PSU) Transportation Research Facility (two ramps), Pleasant Gap, Green Tree, and Freeport. For convenience, these five aggregates were named PSU river pea gravel, PSU crushed aggregate, Pleasant Gap gravel, Green Tree gravel, and Freeport gravel. PSU crushed aggregate was produced by crushing limestone; the others were naturally occurring river gravels. These aggregates were first subjected to gradation and bulk specific gravity tests in accordance with ASTM C 136-84 and C 127-84 test procedures, respectively. Their gradation curves are shown in Figure 1.

PSU river pea, PSU aggregate, Pleasant Gap gravel, Green Tree gravel, and Freeport gravel were formed to have maximum particle sizes of 1.5, 1.0, 1.5, 0.75, and 0.375 in. (38, 25, 38, 19, and 10 mm), respectively. Pleasant Gap, Green Tree, and Freeport gravels also appear to be more uniformly graded than PSU river pea and crushed aggregate. Based on these gradations, their American Association of State Highway and Transportation Officials (AASHTO) grades are 57, 57, 467, 6, and 8 for PSU river pea, PSU crushed aggregate, Pleasant Gap, Green Tree, and Freeport gravels, respectively.

DURABILITY AND ANGULARITY TESTS

Aggregate durability against abrasion was determined by means of the L.A. abrasion test, ASTM C 355-81. For freezing and thawing durability, the test method proposed by Brink (*1*) was followed. The test gravel was subjected to 50 cycles of freezing and thawing in a standard freeze-thaw test apparatus within a temperature range of -15 ± 2°F and 70 ± 2°F. The durations of freezing and thawing were about 3.5 and 1.0 hr,

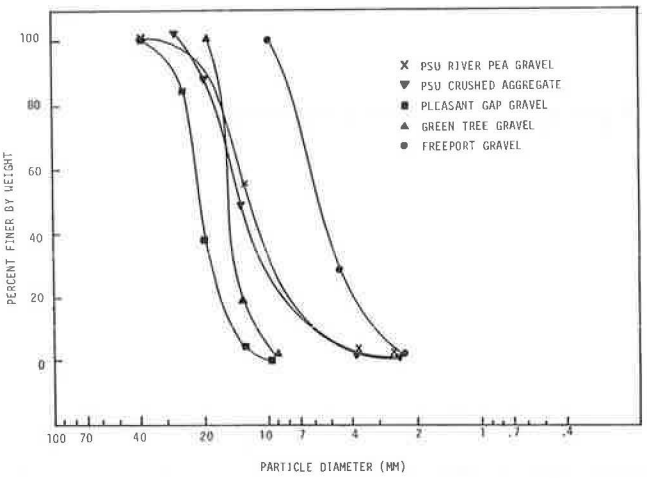

FIGURE 1 Gradation curves of test gravels.

respectively. Test results show that the amount of particle degradation for both PSU river pea and crushed aggregate is very small (less than 2 percent). Because the other gravels were also naturally occurring river gravels and appeared to be as durable as PSU river pea, no freeze-thaw test was performed for these gravels.

Particle angularity was determined by using a metal container 6 in. in diameter and 9 in. in height. For each gravel, particles equal to or larger than the median size were compacted in three equal layers by means of the vibration method. Each layer was subjected to a sustained weight of 5 lbf with a 3-min duration of vibration. The amount of gravel in the container was used to compute the angularity number (AN) from the following equation (*2, 3*):

$$AN = 67 - 100 \times M/(V \times S) \quad (1)$$

where

AN = angularity number,
M = mean mass of compacted aggregate in the cylinder,
V = volume of the cylinder, and
S = specific gravity of the aggregate.

Equation 1, which is available in British Standard 812, is derived from Shergold's work (*4*). It can be shown that Equation 1 can be rewritten as follows:

$$AN = n - 33 \quad (2)$$

where n is the porosity of the aggregate sample. Thus, the AN value indicates the percentage of voids in excess of 33. It should be noted that the AN value reflects the combined effect of angularity, gradation, shape, and surface texture of aggregate particles.

Table 1 summarizes the results of the angularity measurement along with the test results of L.A. abrasion, specific gravity, and gradation. Of the five test aggregates, the angularity number decreases in the order Freeport gravel, PSU crushed aggregate, Green Tree gravel, Pleasant Gap gravel, and PSU river pea.There is no apparent relationship between the angularity number and particle median size or uniformity coefficient.

PARTICLE SHAPE DETERMINATION

The shape of a particle is quantified by measuring its dimensions in three principal axes. For measurement, about 200 particles coarser than the median size were randomly selected. The measurements were obtained first by hand, using a 0.01-in. precision micrometer. This method of measurement is tedious and very time consuming. In addition, because of the irregular particle shape, it is very difficult to obtain dimensions in three directions that are mutually orthogonal.

Primarily due to the tediousness in the method of measurement and the difficulty in obtaining dimensions in the three orthogonal axes, direct hand measurement was later replaced by another method that utilizes the General Electric (G.E.) Optimization II Vision System. In this method, two images of a gravel particle were obtained with a camera, one on the horizontal plane and the other on the vertical plane. From each image, the distance across the particle's outline area was measured every 30 degrees about the centroid. From these measurements, the maximum, minimum, and mean values were obtained. These values were then converted to the actual dimensions across the particle. The entire process,

TABLE 1 GRADATION, SPECIFIC GRAVITY, ABRASION LOSS, AND ANGULARITY NUMBER OF TEST GRAVELS

Test Gravel	Median Size (mm)	Uniformity Coeff.	Specific Gravity	L.A. Abrasion Loss (%)	Angularity Number
PSU River Pea Gravel	12.0 (0.472 in.)	2.0	2.60	20.9	11.7
PSU Crushed Aggregate	12.7 (0.50 in.)	2.4	2.77	19.0	22.7
Pleasant Gap Gravel	20.0 (0.787 in.)	1.5	2.56	35.1	16.0
Green Tree Gravel	15.0 (0.591 in.)	1.3	2.57	25.8	22.5
Freeport Gravel	5.7 (0.224 in.)	1.9	2.62	25.1	24.8

including measurement, conversion, and computation of mean values, was performed on a personal computer.

For each gravel particle, the maximum dimension and the dimension perpendicular to it are obtained from the horizontal view; the smallest dimension is obtained from the vertical view. These values are used as the largest, intermediate, and smallest dimensions of the particle, respectively. Using these dimensions, the particle shape is quantified in terms of sphericity, S, according to the following definition (*2, 3, 5*):

$$S = \sqrt[3]{\frac{bc}{a^2}} \tag{3}$$

where a, b, and c are the largest, intermediate, and smallest dimensions of the particle, respectively.

The value of S ranges between 0 for a flat particle and 1 for a spherical particle. Results of the measurements are presented in the form of a frequency histogram in Figure 2. From these data, the weighted mean sphericity is computed from the ratio of two values; the numerator is the sum of the product of each frequency and its corresponding sphericity, which is taken at the average value of the range, and the denominator is the sum of the frequencies. The computed mean sphericities are 0.70, 0.67, 0.71, 0.70, and 0.82 for PSU river pea, crushed aggregate, Pleasant Gap gravel, Green Tree gravel, and Freeport gravel, respectively. Based on these data, the overall particle shape of Freeport gravel is much closer to spherical than the other gravels; PSU crushed aggregate is the least spherical; and the other three types of gravel, generally speaking, have roughly the same particle shape.

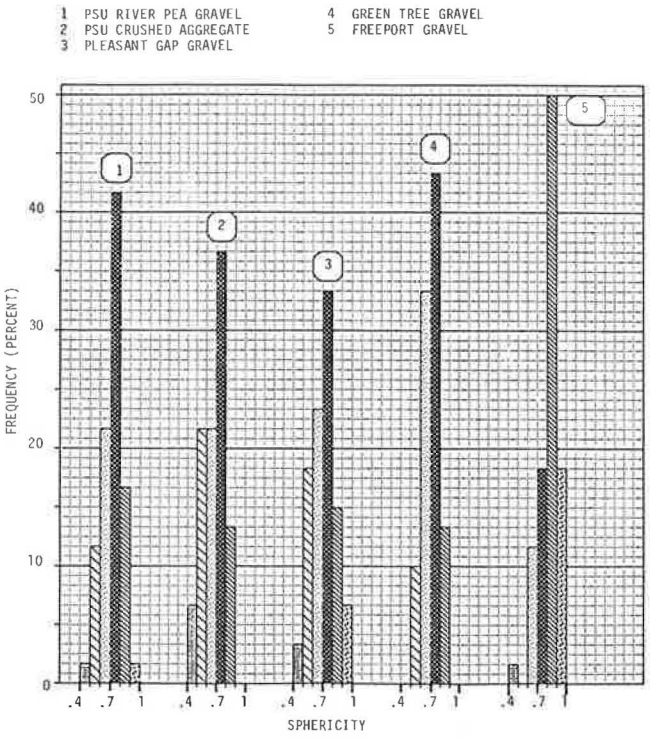

FIGURE 2 Sphericity of test gravels.

DETERMINATION OF SHEARING RESISTANCE

The shearing resistance of the test gravels was determined by means of the triaxial compression test. Two different types of loading were used: static loads and dynamic loads, with the latter used to simulate the moving vehicle loading. The static triaxial test is the method that is normally adopted, and the dynamic triaxial test is performed to determine the effect of loading rate (or deformation rate) on shearing resistance.

The static triaxial compression test was conducted using an apparatus composed of a standard volume-change measuring device and a triaxial cell specially designed and constructed to accommodate a specimen 9 in. in diameter by 19 in. in height. A universal testing machine was used to apply axial loading at a deformation rate of 0.05 in./min. The applied load was read directly from the machine, whereas the specimen deformation was measured by using a 0.001-in. dial gauge.

A metal mold 9 in. in diameter and 19 in. in height, split into two equal sections lengthwise, was used to fabricate the test specimens. Loose specimens were prepared by pouring the gravel into rubber membranes that were stretched inside the mold. To prepare denser samples, the gravels were deposited in three layers, and each layer was rodded by hand to a desired density. Each specimen required about 80 lb of gravel. Because of the large size and heavy weight of the specimens, two persons were needed to perform the testing.

A suction of about one atmosphere was applied to the gravel sample with a vacuum pump to make the specimen stand up without support. The split mold was removed and the triaxial cell was assembled. Then the cell was filled with water until the sample was completely submerged and the desired confining pressure was applied. Immediately after the confining pressure was applied, the vacuum inside the specimen was turned off. The test specimen was then saturated with de-aired water.

The test was performed on specimens of three levels of relative density. For each relative density, the specimen was subjected to three levels of confining pressure—10, 20, and 30 psi. At least two tests were performed for each test condition. If the results of the two tests differed by more than 5 percent, a third test was performed.

From triaxial compression test results, the Mohr-Coulomb failure envelope for each level of relative density was plotted. For all of the aggregates tested, the failure envelopes passing through the origin are slightly curved downward. The curved failure envelope, which is typical for granular materials, can be attributed to particle breakdown under higher confining pressures (*6*). These envelopes are approximated by straight lines to obtain shear strength parameters. Table 2 summarizes the internal friction angle and cohesion thus obtained. The results show that the internal friction angle is highest for PSU crushed aggregate and lowest for Pleasant Gap gravel.

The dynamic triaxial compression test apparatus consists of a loading device and a recording system. The loading device, which is composed of a loading mechanism and a reaction frame, was specially designed and constructed. The loading mechanism (Figure 3) is operated under the same principle as that of Olson and Kane (*7*). The dynamic load is applied by means of nitrogen gas, which is supplied by a high pressure tank. The required amount of nitrogen gas is regulated and

TABLE 2 INTERNAL FRICTION ANGLE AND COHESION OBTAINED FROM STATIC AND DYNAMIC TESTS

Aggregate Test	Static Load, Relative Density (%)						Dynamic Load, Deformation Rate (in/sec)							
	25		50		75		20		40		60		80	
	ϕ^*	C**	ϕ^*	C**	ϕ^*	C**	ϕ^*	C**	ϕ^*	C**	ϕ^*	C**	ϕ^*	C**
PSU Pea Gravel	35	4	41	2	44	2	39	1	40	1	36	1	36	2
PSU Crushed Aggregate	38	2	40	2	43	2	41	1	40	1	40	1	40	1
Pleasant Gap Gravel	27	8	30	7	31	9	30	4	32	4	30	3	32	3
Green Tree Gravel	29	7	30	9	32	10	31	4	31	3	33	2	31	4
Freeport Gravel	33	5	34	6	35	6	34	3	34	2	33	2	34	2

*Internal friction angle in degrees.
**Cohesion in psi.

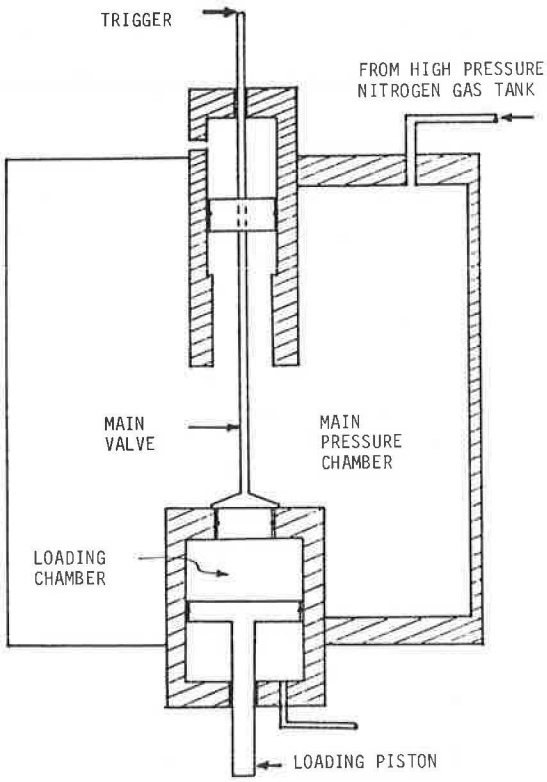

FIGURE 3 Schematic view of dynamic loading mechanism.

stored in the main pressure chamber. When the loading mechanism is activated by a sudden pull of the trigger, the plug that blocks the main port is lifted rapidly and the gas rushes into the loading chamber. This pushes the loading piston downward at a very high speed and induces the desired vertical loading in the test specimen.

To satisfy safety requirements, the pressure chamber is surrounded by 4-in. × 4-in. studs that are nailed together with two metal strips, and the triaxial cell is enclosed in a metal cage. The cage is made of expanded steel and has a door on one side so that the test specimen in the triaxial cell can be pushed in and out of the cage.

The vertical (axial) load applied to the test specimen was measured with a type C3P1 load cell, manufactured by BLH, Inc. with maximum capacity of 10,000 lb. The load cell was placed on top of the loading cap, which rested on top of the test specimen. The load cell was connected to a 12-volt amplifier, which was set at an amplification factor of 500.

Test specimen deformations were measured with a linear potentiometer, type M1326-2-502, with a capacity in ohms of 5K ± 5 percent and measuring up to 2 inches, purchased from Maurey Instruments. The housing of the linear potentiometer was attached to a steel rod about 0.5 in. in diameter by 6 in. in length, which was in turn clamped perpendicularly to one of the triaxial cell's supporting rods. The core of the linear potentiometer rested vertically on the top of the test specimens.

Both the load cell and the linear potentiometer were connected to a SOLTEC Visigraph-5L electronic recorder. The recorder can accommodate a maximum chart speed of 200 cm/sec.

The dynamic tests were performed only for one level of relative density, which was as close to the loosest condition of the gravel as possible. This relative density level was used to simulate the density condition of the gravel in the arrester bed. For this level of density, the test specimen was subjected to three levels of confining pressure applied through a vacuum; they were 5, 10, and 12.5 psi. The maximum pressure of 12.5 psi was used because it was the highest vacuum the available vacuum pump could produce.

The compressive strength of PSU pea gravel thus obtained is plotted against deformation rate in Figure 4. It is seen that as the rate of deformation increases, the compressive strength decreases from the static value to a minimum, then increases slightly. All other aggregates also exhibit a similar trend. The shape of the curve roughly resembles the trend obtained by Whitman from his study on sands (*8*). According to Whitman, the decrease in compressive strength with increasing deformation rate can be attributed to the effect of kinetic friction, which is generally less than the static friction. The increase of compressive strength at a very high deformation rate can be explained by the fact that the interlocking among particles becomes more effective when the particles are not given sufficient time to find the easiest path to pass one another.

From these dynamic strength data, the failure envelopes are plotted. As with the static failure envelope, the dynamic

failure envelope is also slightly curved downward. Using the straight line approximation, the internal friction angle and cohesion for different deformation rates are obtained and are summarized in Table 2. It is seen that within the deformation rates tested, the internal friction angle fluctuates slightly with the deformation rate. The data reveal no definite trend of variation, and therefore the data fluctuation could be attributed to possible testing errors and linear approximation of the failure envelopes.

AGGREGATE PERFORMANCE

Except for the Green Tree gravel, field performance of the test aggregates has been studied by Wambold et al. (*9*). They conducted extensive field testing to investigate deceleration, stopping distance, and various other important parameters of aggregate performance in the arrester bed. The test was conducted with a wide range of entry speeds and also with different aggregate layer thicknesses for PSU river pea gravel. The average deceleration data, according to their test results, are tabulated in Table 3. The mean value of deceleration for each aggregate is computed for ease of comparison, because the data are widely scattered and no well-defined trend of variation of deceleration with entry speed similar to that detected by Cocks and Goodram (*10*) can be found. Because there is no clear trend of how deceleration varies with layer thickness, the PSU river pea gravel data are combined into two levels of thickness in the table.

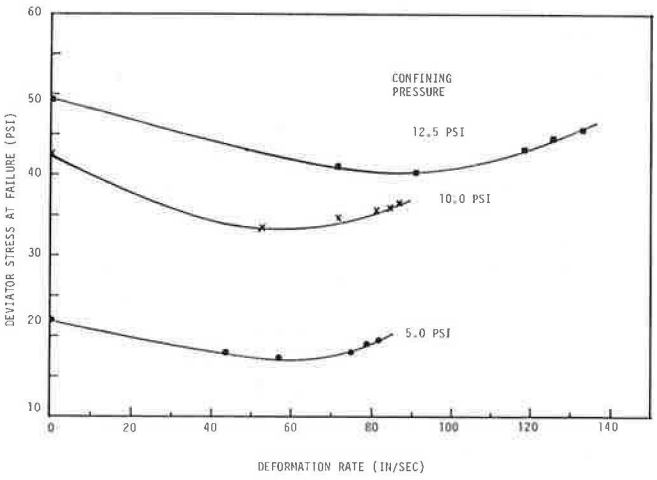

FIGURE 4 Deviator stress at failure versus deformation rate for PSU river pea gravel.

For dump truck data, the deceleration value of Pleasant Gap gravel was obtained only from one test. Because of the wide scattering of the data, a direct comparison of this value with other data should be made with caution. The dump truck deceleration data clearly indicate that the performance of PSU crushed aggregate is considerably lower than the river pea gravel. Meanwhile, the three types of gravel, generally speaking, perform equally well, although Pleasant Gap gravel slightly outperforms the other two for tests with a dump truck, and Freeport gravel performs a little better than the others for a tractor-trailer.

In the arrester beds, the moving trucks induce dynamic shearing to the aggregate. Thus, to evaluate the effect of shearing resistance on aggregate performance, the dynamic internal friction angle and cohesion should be used. Furthermore, because there are some resemblances between the process of a wheel sinking into aggregate and the bearing capacity failure of a shallow foundation, the bearing capacity principle has been used to evaluate the resistance of soft ground to moving vehicles (*11*). The bearing capacity of each aggregate is computed using the following equation (*12*):

$$q_o = cN_c + qN_q + (1/2)\gamma BN_\gamma \quad (4)$$

where

q_o = bearing capacity,
c = cohesion,
q = surcharge pressure,
γ = unit weight of aggregate, and
B = width of wheel.

TABLE 3 AVERAGE DECELERATION DATA (*9*)

Vehicle Type	Test Aggregate	Aggregate Thickness (in.)	Entry Speed (mph)	No. of Test	Average Deceleration (g) Range	Mean
Dump Truck	PSU River Gravel	18 - 22	29 - 54	11	0.26 - 0.48	0.38
		30 - 36	39 - 47	8	0.45 - 0.59	0.52
	PSU Crushed Aggregate	15 - 18	29 - 47	10	0.20 - 0.33	0.26
	Pleasant Gap Graval	96	50	1	0.57	0.57
	Freeport Gravel	72	39 - 54	5	0.45 - 0.56	0.50
Tractor Trailer	PSU River Gravel	36	40 - 51	6	0.29 - 0.44	0.36
	Pleasant Gap Gravel	96	48	2	0.37 - 0.39	0.38
	Freeport Gravel	72	47 - 60	4	0.37 - 0.52	0.42

N_c, N_q, and N_γ are bearing capacity factors that are functions of internal friction angle (ϕ) as follows:

$$N_c = (N_q - 1) \cot \phi \quad (5)$$

$$N_q = e^{\pi \tan \Phi} \tan^2(45° + \phi/2) \quad (6)$$

$$N_\gamma = 2(N_q + 1) \tan \phi \quad (7)$$

For a wheel width of, say, 2 ft with no surcharge pressure, the bearing capacities computed from the internal friction angle and cohesion obtained under the 80 in./sec deformation rate are approximately 177, 185, 137, and 125 psi for PSU river pea, PSU crushed aggregate, Pleasant Gap gravel, and Freeport gravel, respectively. PSU crushed aggregate thus has the highest bearing capacity. Because of the high bearing capacity, the depth of wheel penetration into the aggregate will be small. As a result, the drag force and hence the mean average deceleration will be low, as indicated in Table 3.

The difference in bearing capacity between PSU river pea and PSU crushed aggregate is smaller than the differences among PSU river pea, Pleasant Gap, and Freeport gravels. There is a rather small difference in bearing capacity between PSU river pea and crushed aggregate but a significant difference in the mean average deceleration. The fairly equal deceleration value among the three gravels can hardly be explained. This result suggests that the analysis of shearing resistance alone is not sufficient to determine the aggregate performance in the arrester bed.

The data show that the gradation of PSU crushed aggregate is nearly the same as river pea gravel, but the crushed aggregate has particles less spherical and more angular than the river pea gravel. The less spherical particle shape and higher particle angularity appear to be important factors in causing smaller deceleration values for the crushed aggregate.

Comparing the PSU river pea, Pleasant Gap, and Freeport gravels, Pleasant Gap gravel has the largest median particle size and lowest uniformity coefficient (i.e., most uniform), while Freeport gravel has the smallest median size with a uniformity coefficient approximately equal to that of PSU pea gravel. The angularity number is highest for Freeport gravel and lowest for PSU pea gravel. In short, Pleasant Gap gravel is most uniform, PSU pea gravel is least angular, and Freeport gravel is most spherical. Thus, the nearly equal field performance of the three gravels should reflect more the combined effect of gradation, angularity, and sphericity than just the effect of interparticle friction and cohesion. Unfortunately, no data are available to determine the effect of each of the factors on field performance of the test aggregates. As a result, no recommendation can be made at present regarding a set of values which can be used as a guide for selecting aggregate.

SUMMARY AND CONCLUSIONS

Gravel arrester beds are often installed along long steep downgrades to stop runaway trucks. In the arrester bed, the gravel must have adequate properties to maintain the desired function of the bed. This paper presents test methods, results of testing of five aggregates, and field performance of the aggregates.

The five test aggregates were obtained from existing arrester beds throughout Pennsylvania. They are PSU river pea gravel, PSU crushed aggregate, Pleasant Gap gravel, Green Tree gravel, and Freeport gravel. Tests performed were gradation, bulk specific gravity, L.A. abrasion, and freeze-thaw tests. Also, particle angularity, sphericity, and shearing resistance were determined. The testing was conducted in accordance with standard procedures when available. In the determination of particle angularity, Shergold's method was adopted; particle shape was measured by using the G.E. Optimization II Vision System; and shearing resistance was determined using both static and dynamic triaxial test methods.

Of the five aggregates tested, Pleasant Gap gravel has the largest and Freeport gravel the smallest median particle size. Green Tree gravel has the most uniform and PSU crushed aggregate the least uniform gradation. The angularity number is largest for Freeport gravel and smallest for PSU river pea gravel. Freeport gravel particle is most spherical and PSU crushed aggregate least spherical. The static internal friction angle is highest for PSU crushed aggregate and lowest for Pleasant Gap gravel.

Except for Green Tree gravel, field performance of the other aggregates is available for comparison. The performance is evaluated in terms of mean average deceleration value. The available data indicate that PSU crushed aggregate performs least well among the four; the poor performance can be attributed to its high internal friction angle, high angularity number, and less spherical particles. The other three aggregates perform almost equally well, although the bearing capacity differs significantly among the three gravels. This observation strongly suggests that aggregate performance in the arrester bed depends not only on interparticle friction and cohesion but on particle gradation, angularity, sphericity, and possibly other factors as well. Because the available data are not sufficient to determine the individual effect of these factors on aggregate performance, it is not possible at present to recommend a set of values to be used as a guide for selection of arrester bed material.

Based on the results of this study, it can be concluded that aggregate gradation and interparticle friction are not sufficient to determine performance in the arrester bed. Factors such as particle angularity and sphericity also greatly influence aggregate performance. Moreover, for long-term performance, particle durability is a dominant factor. Therefore, testing of aggregate for use in the arrester bed should involve determinations of not only gradation and interparticle friction but also angularity number, sphericity, and durability.

ACKNOWLEDGMENTS

This study was sponsored by the Pennsylvania Department of Transportation in cooperation with the Federal Highway Administration; their financial support of the study is gratefully acknowledged. The laboratory testing was conducted by W. P. Liao, N. Hallak, and I. Al-Qadi. The particle sphericity measurement was made through the assistance of J. C. Wambold. All of their efforts are greatly appreciated.

REFERENCES

1. R. H. Brink. Rapid Freezing and Thawing Test for Aggregate. *Bulletin 201*, HRB, National Research Council, Washington, D.C. 1958, pp. 15–23.
2. M. A. Ozol. Shape, Surface Texture, Surface Area, and Coatings. In *Significance of Tests and Properties of Concrete and Concrete-Making Materials*, ASTM *Special Technical Publication 169 B*, American Society for Testing and Materials, Philadelphia, 1978, pp. 584–628.
3. D. F. Orchard. Properties and Testing of Aggregates. In *Concrete Technology*, 3rd ed., John Wiley and Sons, Inc., New York, 1976.
4. F. A. Shergold. The Percentage Voids in Compacted Gravel as a Measure of Its Angularity. *Magazine of Concrete Research* (London), Vol. 5, No. 13, August 1953, pp. 3–10.
5. B. Mather. Shape, Surface Texture, and Coatings. In *Significance of Tests and Properties of Concrete and Concrete Aggregates*, ASTM Special Technical Publication No. 169, American Society for Testing and Materials, Philadelphia, 1966, pp. 284–292.
6. T. W. Lambe and R. V. Whitman. *Soil Mechanics*. John Wiley and Sons, Inc., New York, 1969.
7. R. E. Olson and H. Kane. Dynamic Shearing Properties of Compacted Clay at High Pressures. *Proc., 6th International Conference on Soil Mechanics and Foundation Engineering*, Vol. 1, 1965, pp. 328–332.
8. R. V. Whitman. The Response of Soils to Dynamic Loading. Report 26. U.S. Army Engineering Waterways Experiment Station, Vicksburg, Miss., May 1970.
9. J. C. Wambold, L. Rivera, and M. C. Wang. A Field and Laboratory Study to Establish Truck Escape Ramp Design Methodology. Report FWHA-PA-86-032 + 83-26, Final Report, PTI 8617. The Pennsylvania Transportation Institute, Pennsylvania State University, 1986.
10. G. C. Cocks and L. W. Goodram. The Design of Vehicle Arrester Beds. *Proc., The Eleventh ARRB Conference*, University of Melbourne, Part 3, Volume 11, 1982, pp. 24–34.
11. J. Y. Wong. *Theory of Ground Vehicles*. John Wiley and Sons, Inc., New York, 1978.
12. K. Terzaghi and R. B. Peck. *Soil Mechanics in Engineering Practice*, 2nd ed. John Wiley and Sons, Inc., New York, 1967.

Salt Weathering of Limestone Aggregate and Concrete Without Freeze-Thaw

CARL F. CRUMPTON, BARBARA J. SMITH, AND G. P. JAYAPRAKASH

Kansas aggregates are frequently alkali reactive or subject to D-cracking when used in concrete. The use of deicing salt, usually halite (NaCl) in Kansas, makes those problems worse. Salt allows the concrete to become wet and to stay wet longer, increasing the time for reactions to occur. Clays in limestone aggregates have been altered by deicing salt solutions remaining in the aggregates. Degraded illite changed to sodium montmorillonite. Quartz has been altered by electric currents induced in the concrete. Some quartz took on an optical property, undulatory extinction, that is frequently associated with potential alkali reactivity. Salt (NaCl) scaling of concrete blocks and slabs without freeze-thaw has been observed. Monitoring salt water movement through the walls of concrete cups has provided insight on how and where salt water moves in concrete. The salt water movement and deposition of salt crystals has caused considerable scaling of both the cement paste and the limestone aggregates of the concrete. The salt "gnaws away" or corrodes the limestone aggregate and cement paste, attacking the most accessible and most susceptible parts first. Particles as large as 0.6 in. have scaled from limestone aggregates. Most of the scaled flakes are oatmeal size and no larger than 0.2 in. in length. A silane "sealer" did not prevent salt water from moving through the limestone aggregates in the concrete cups. All three cups treated with silane cracked on the first salt treatment cycle (five days filled with salt water, emptied, soaked in plain water, then nine days of air drying). Untreated cups did not crack even after 12 cycles. No freeze-thaw was involved.

Unlike many states, Kansas does not have an abundance of good native mineral aggregates for concrete and therefore must make do with what is available. Sand, sand-gravel, and crushed limestone are the three most commonly available Kansas aggregates. The state uses the crushed chat (chert) tailings from the lead and zinc mining operations in southeast Kansas. Gravel, crushed sandstone, and silicified chalk have been used. Expanded shale, a man-made, lightweight, glassy aggregate that is highly porous, resembling scoria or pumice, has also been used.

Gravels, sand-gravels, and sand may contain reactive quartz, glassy volcanics, opaline, chalcedonic, cherty, or other particles that are alkali reactive. The silicified chalk is quite variable and frequently contains reactive opaline and low christobalite-tridymite material. Silica-cemented sandstone may also be reactive due to the same substances. The calcite-cemented sandstone, sometimes locally called quartzite, is usually not reactive, but in places the cement is dolomitic, which may cause problems through the alkali-carbonate dedolomitization process. A few beds of fine-grained dolomite have been used as crushed stone, and they too suffer that reaction. The expanded shale aggregates are sometimes prone to an alkali-aggregate reaction that has caused growth of bridge decks. Many lightweight decks had several inches of length (as much as 14 in.) sawed off to accommodate the expansion reaction and growth. Most Kansas limestone units contain beds that produce D-cracking under freeze-thaw conditions. Some gravel and sand-gravel sources have contributed to D-cracking.

Because of all their mineral aggregate problems, Kansas expended considerable effort during the 1930s, 1940s, and 1950s sorting out sources of acceptable and unacceptable material for concrete. The strategy became one of avoiding reactive or untested sources of potentially reactive aggregates, or requiring replacement of 30 to 35 percent of the coarse aggregate fraction with crushed limestone—a process called sweetening (*1*).

About 30 years ago Kansas began using deicing salt regularly. It was soon recognized that deicing salt was aiding and abetting concrete deterioration. Alkali-aggregate reaction and D-cracking came on quicker than before salt was used. By then, however, its use to provide bare pavements had become entrenched in the traveling public's mind. Salt continued to be used as a "safety agent" no matter what researchers, materials engineers, or environmentalists said about the detrimental effect of salt on bridges, pavements, or the roadside and subsurface environment. Reevaluation of materials became necessary. There was controversy over whether the problems were primarily physical, chemical, both, or neither. Some maintained that there was no problem. Yet many concrete roads and bridges were rapidly decaying. There was no lack of deteriorated concrete to study. The financial burden to repair or replace prematurely damaged roads, bridges, roadside plantings, and water wells across the country is strongly felt by taxpayers and public servants alike.

CLINICAL OBSERVATIONS

Several observations have been made relating to the various ways salt seems to affect Kansas mineral aggregates and the concrete containing them. This report does not address salt-induced corrosion of reinforcing steel. Salt is hygroscopic and absorbs moisture from humid air. This enhances the alkali-aggregate reaction, which generally does not proceed if the

C. F. Crumpton, 4728 S.W. 18th Terrace, Topeka, Kans. 66604. B. J. Smith, Kansas Department of Transportation, Topeka, Kans. 66612. G. P. Jayaprakash, Transportation Research Board, National Research Council, Washington, D.C. 20418.

internal relative humidity of the concrete is below about 80 percent (*1*). When enough salt is present, the concrete can become saturated at relative humidities below 80 percent (*2*).

Even in the reasonably dry Kansas environment the near-ground atmosphere usually contains considerable moisture during the early morning hours, before the hot sun begins surface evaporation. During the day the exposed surfaces dry as the early morning dew evaporates. The internal moisture in the concrete is slow to leave. Salt increases the dwell time for moisture in the concrete. This gives added time for the alkali-aggregate reactions to proceed as the concrete warms in the sun. Hence salt increases the chances for concrete to become wet and stay wet internally. If the concrete contains reactive aggregates, the chances for reaction are increased. Salt also provides almost daily cycles of surface wetting and drying, as well as warming and cooling of exposed concrete. Alkali chloride deicing salts can add alkalies to the concrete (*3*) to further aggravate the reaction problem.

Alkali-carbonate reactions were observed to occur in a four-year-old Kansas concrete pavement. The pavement had been built using a crushed stone coarse aggregate composed of a fine-grained dolomite. The pavement was near Kansas rock salt mines and was deiced regularly during the winter with the local rock salt. Stains and surface dampness were frequently observed near sawed transverse joints, especially at their intersection with longitudinal joints. Cores obtained in those locations revealed little sign of internal cracking or deterioration. However, the copper nitrate staining technique recommended by Dolar-Mantuani (*3,4*) revealed that the fine-grained porous dolomite was inverting to calcite in the border or rim areas of the dolomite aggregate. After a few more years the joints required repair because they had begun to deteriorate.

Salt was helping maintain a high internal humidity. During the warm months an alkali-carbonate dedolomitization reaction was occurring. This was augmented by D-cracking of the same aggregates during the winter. The sand-gravel used with the dolomite was not observed to be reactive. This fact, and the fact that the concrete contained only 36 percent crushed dolomite, allowed the road to be maintained for most of its 20-year design life by repairing the joints as deterioration progressed. Some blowups occurred on hot days after rain.

A report of a Kansas example of map cracking progressing into D-cracking in a limestone-sweetened reactive aggregate concrete pavement was published by TRB several years ago (*5*). Deicing salt exacerbated the problem with alkali-aggregate reaction and pavement blowups occurring during the warm months and D-cracking during the winter. At the end of 11 years only 3 percent of the joints were still good. Map cracking, D-cracking, and pavement blowups are all enhanced by the hygroscopic action of salt, which absorbs moisture from the air and keeps the concrete more saturated.

Hudec and Rigby (*6*) found that immersing carbonate aggregates in a 3 percent sodium chloride solution doubled their later water absorption at 30°C and 98 percent relative humidity, compared to unsalted specimens. Under immersion conditions the degree of saturation increased an average of about 13 percent for the salted rocks. Many of the individual rock samples showed considerably more or less than the average increase. Hudec and Rigby found little effect at 45 percent relative humidity. They did not report any other levels of relative humidity tests.

Under conditions of wetting and drying, warming and cooling, or freezing and thawing, the water inside the concrete and its porous aggregates shifts from small spaces to larger spaces, from the inside to the surface, and from pores to cracks. When the conditions reverse, the movement of moisture also reverses direction. Thus the moisture in the concrete moves about with changes in temperature, humidity, wind velocity, vapor pressure, rainfall, sunshine, electrical current, and so forth.

As the water moves, it dissolves or deposits substances depending on internal conditions. On a microscopic level, conditions inside salted, moist concrete seem to be continually changing with changing ambient conditions. When moisture moves between paste and limestone aggregates, the border zone of each is somewhat altered. The aggregate may develop negative or positive rims (*3,7,8*) that are often made up of multiple layers. Air voids, cracks, and other voids in concrete also frequently contain multilayered coatings inside the voids, attesting to many alternating cycles of water movement and deposition due to changing conditions. Any petrographer who has examined much in-service concrete has observed these deposits.

Efflorescence or fibrous deposits on the external surfaces of concrete often give clues to changing internal conditions that may involve the mineral aggregates. Such was the case of soft, fluffy, fibrous, white deposits collected from the bottom of an old bridge deck. Hot mix asphalt covered the four-lane bridge deck, which was being evaluated for probable replacement. X-ray, microscope, and chemical studies of the soft white deposits revealed that they were aphthitalite $(K,Na)_2SO_4$ with thernardite $NaSO_4$.

The deck had been routinely deiced with rock salt that contained from 2 to 7 percent sulfate, present mostly as anhydrite (*9*). Thus the sodium sulfate was not surprising. However, there was little potassium in the deicing salts tested, and the authors therefore believed the potassium must have been derived from concrete constituents. They found that the limestone aggregates in the concrete above the fibrous deposits were often badly deteriorated. Bukovatz et al. described the concrete as a "sea of deterioration" with occasional "islands" of sound concrete (*10*, Figure 4). X-ray studies of the clay fraction of the cracked and broken limestone aggregates revealed that much of the degraded illite normally present had altered to sodium montmorillonite. Sodium from the NaCl had exchanged with potassium in the degraded illite. It was concluded that most of the potassium in the aphthitalite was from that source. There were indications that alkali-feldspars in those "seas of deterioration" were also weathering under the highly saline freeze-thaw conditions created by deicing salts penetrating the badly cracked hot mix asphalt overlay to the old non-air-entrained concrete below. The concrete seldom had a chance to dry out thoroughly because the hot mix retarded moisture evaporation more than its penetration.

Kansas Department of Transportation (KsDOT) researchers have studied the effect of salt on indoor and outdoor exposures of concrete blocks and slabs for many years (*9, 11–15*). Most of that work involved freeze-thaw cycling, so the effect of salt alone could not be separated from that of freeze-thaw. In some instances, however, observations were recorded that indicated salt caused scaling before any freezing cycles had occurred (*13*).

In electro-migration studies of salt in concrete (*14,15*) it was noted that the salt ions moved through the cement paste,

not through carbonate aggregates. Other studies (*11*) noted that the sodium in salted concrete was sometimes highest in the paste and sometimes highest in the limestone aggregate. An added "clinical observation" from the electro-migration studies of salt movement (*14,15*) was not included in the reports but was mentioned in an in-house memo. It was observed in petrographic studies of the electro-treated salty concrete that much of the quartz had taken on an optical characteristic often associated with alkali-reactive quartz, namely undulatory extinction. If, through electrical treatment, the quartz had become reactive, it could imply a long-term durability loss for electro-treated concrete or perhaps even concrete struck by lightning. A discussion of reactive quartz and undulatory extinction may be found in a recent work by Dolar-Mantuani (*3*).

In other unreported KsDOT work, the authors pursued scaling studies of concrete blocks subject to surface salting under outdoor exposure. The blocks contained no reinforcing steel and were made such that one-half of each block contained air-entrained concrete and the other half contained non-air-entrained concrete of the same mix. Companion blocks were made for exposure without salt applications. The cured blocks were 75 days old when they were moved outdoors in late spring of 1983 after all danger of frost was past (all blocks were supported on wooden frames). When the blocks were three months old, 300 ml of a 3 percent NaCl (laboratory grade) solution was applied three times a week to the test blocks. The same amount of salt-free water was applied to the companion control blocks at the same time.

During the first week it was necessary to spread the liquids on the block surfaces because they tended to bead up and not flow over the concrete. After the first week (three treatments) the salt solution quickly spread over the entire surface of the blocks when applied. The plain water continued to bead up and required spreading effort by rubber spatula to cover the block surface. It was noted that the salt-treated blocks took far more time to surface dry than did the blocks treated with water. As treatments progressed, the surface drying time differential increased.

After nearly five months of outdoor exposure, 49 salt applications had been made but no freezing had occurred. All of the salt-treated blocks had very shallow surface flaking, whereas the control blocks treated only with water did not. The air-entrained portion of the salt-treated blocks had slightly less surface scaling than did the non-air-entrained portions. The 49 salt applications would roughly equate to 2½ years of Kansas road salting, according to McCollom (*16*). There would not be 2½ years of road salting without freeze-thaw in Kansas, however. At an average of more than 68 freeze-thaw cycles per winter in Kansas, 2½ years of salting would represent about 170 cycles of freeze-thaw. Another difference in these tests is the lack of sulfates and other impurities normally present in Kansas rock salt. The salting of the blocks continued through the winter months and the scaling increased considerably but mostly in the non-air-entrained half of the salt-treated blocks.

SALTY CONCRETE CUPS

In 1986 the authors began a study of salt movement in concrete by using cored concrete cups (*17–19*). They were already studying salt variations in adjacent concrete samples (*20*). Salt crystal growths in concrete (*21,22*) and simpler or more rapid means of determining salt content in concrete (*23,24*) were topics of other salt studies in KsDOT labs.

For making concrete cups (Figure 1), two concentric cores are taken in the concrete. The smaller, shallower inner core is drilled first and broken out before the larger outer core is drilled to a greater depth—often through the full thickness of concrete (*17*). The cored cups are rinsed and allowed to air dry before being used for salt movement studies. In order to obtain cups with walls ⅜ in. thick, the authors used a core bit with a 2¼ in. outside diameter for the inner core or "well" of the cup. The larger core bit is 3 in. in inside diameter. Other sizes and combinations may be used. For variable thickness walls the authors used a bit of 4 in. inside diameter for the larger core. By offsetting the larger core to one side of the inner core, they obtained cup walls that range from ⅜ in. to about 1½ in. thick in the same cup. All cups have a bottom from ½ in. to several inches thick.

A 15 percent salt solution made from standard Kansas deicing salt was used. This concentration was chosen because it was used in the NCHRP 244 studies (*25*). It is also the concentration used many decades ago for NaCl durability studies of limestones (*26*). It was reported that Indiana limestone suffered seven times as much deterioration from the salt durability tests as from freeze-thaw action. In the present studies, the 15 percent salt solution was used to fill the concrete cups to within about ½ in. of the top.

Moisture may show up on the outside of the cup in a matter of minutes (2 to 20 minutes), but it is usually several hours to a day before salt crystals are deposited on the outside of the concrete cup (*17–19*). Figure 2 shows the outside of a cup nearly two weeks after salt water was added. There are NaCl crystal deposits at the perimeter of many of the limestone aggregates. Aside from cracks, the coarse limestone aggregate border is the zone of most rapid salt movement. Some of the limestone particles become coated with salt, indicating more rapid flow through certain aggregates than through others. Earlier work with field concrete revealed a sodium chloride buildup in some of the limestone coarse aggregates in a bridge deck (*11*). In studies of D-cracking in Kansas concrete pavements, the authors often observed from core samples that many aggregates were sound and that only a portion of the limestone coarse aggregates were deteriorating. Those were the most susceptible aggregates. The authors now wonder if our salt cup tests are identifying some of those most susceptible individual aggregate particles.

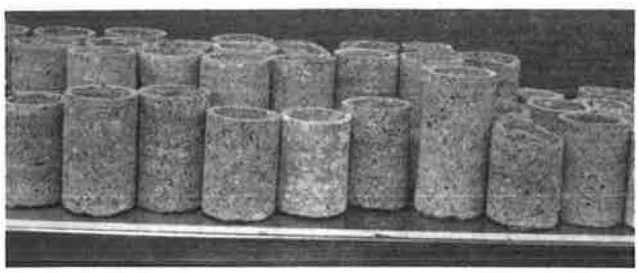

FIGURE 1 A group of concrete cups made by taking two concentric cores such that the cup walls are about ⅜ in. thick and the bottom is at least ½ in. thick.

The photograph in Figure 2 also shows general surface dampness on the outside of the cup. This is moisture adsorbed from the air. On humid days the salt drew the moisture from the air and the cup surface remained damp as long as the humidity was high. This did not occur on untreated cups. On days when it was raining outdoors, the moisture buildup on the outside of the cups was often great enough to dissolve some of the salt deposits. The water ran down the outside of the cups and collected in the glass plates containing the cups. Thus, periods of very high humidity sometimes obliterated the original depositional pattern of the salt on the outside of the cups.

At the top of the cup in Figure 2 is a mass of salt around the inside perimeter. This is from salt water wicking up the inside walls, evaporating, and leaving the halite crystals behind. Figure 3 shows this buildup in an early stage. Rounded masses of halite crystals appear first. Needle crystals of salt then often grow from those masses. More massive crystals begin to grow on the needles. As evaporation continues, the entire inside perimeter at the top of the cup becomes coated with the salt deposit, as seen in Figure 2. The needles are eventually completely overgrown and no longer show as salt deposition continues.

When salt water came through the walls of the cup, halite crystals also grew on the outside of the cup. Small oatmeal-sized flakes of paste and aggregates scaled from the cup's outside surface. Figure 4 shows a cup before salt treatment. Note especially the two limestone aggregates near the top of the cup to the left of the letter H. Figure 5 is a close-up of the larger of those two aggregates after salt treatment. Notice the surface cracking and thin flakes pushing out of that aggregate. Salt crystals are growing below the surface and causing surface flaking or scaling. Figure 6 shows the same aggregate after the surface had flaked off and the salt deposits were dissolved by gentle immersion of the emptied cup in plain water.

FIGURE 2 A concrete cup which has been filled with a 15-percent solution of deicing salt. The salty water has moved through the cup walls primarily at the border of limestone aggregates and has left salt deposits there as the water evaporated. The salt often draws moisture from air and leaves the surface damp on humid days.

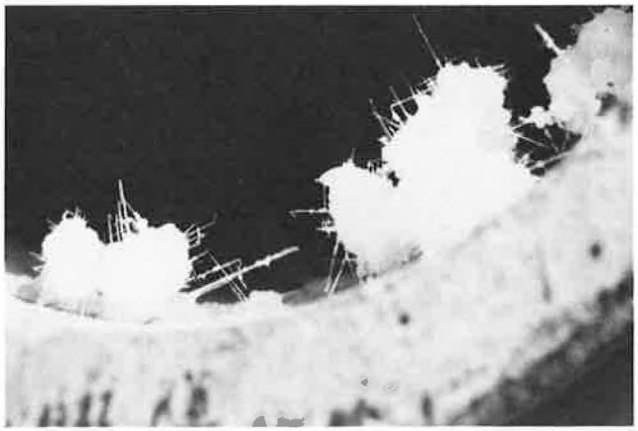

FIGURE 3 Salt crystal deposits and fibers on the inside top of a cup. These formed from salt water wicking up the inner walls and evaporating.

FIGURE 4 A concrete cup before any treatment with salt water. Note the two limestone aggregates at the top just to the left of the letter H.

The authors cycled the first two cups through a dozen salt water treatments. Each cycle consisted of five days with 15 percent salt water in the cups, followed by emptying, gentle soaking in plain water to remove the salt deposits, and air drying for nine days. More oatmeal-sized flakes were dislodged by the salt crystal growths during each cycle. Figure 7 is a close-up of some clumps of those flakes, the largest of which is 0.2 in. long. Figure 8 shows the largest individual scaled flake collected, which is 0.6 in. in length. The flake is

FIGURE 5 The larger of the two aggregates noted in Figure 4. Salt has moved through the aggregate, depositing near its top surface. The salt is also pushing thin flakes from the surface of the aggregate.

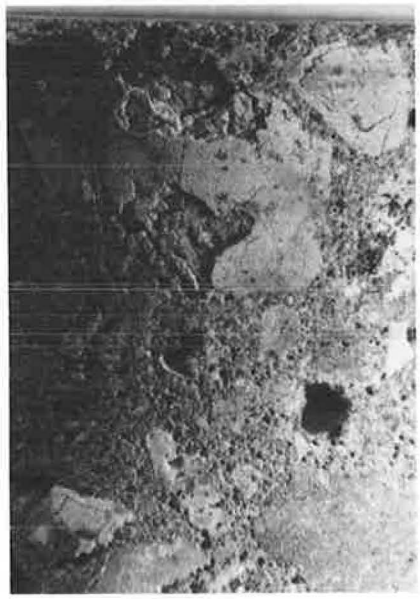

FIGURE 6 The aggregate particle in Figure 5 after the salt has scaled away part of the surface. A distinct rim shows in the second aggregate slightly above and to the right. The limestone in the rim has been separated from the aggregate particle by salt weathering.

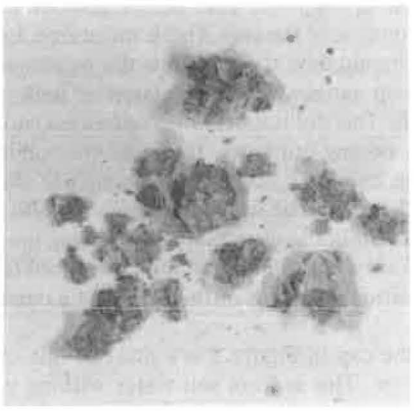

FIGURE 7 Typical scaled particles of paste and limestone aggregates. These range up to 0.2 in. in longest dimension.

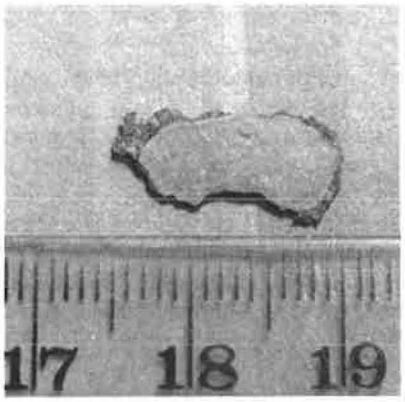

FIGURE 8 A bean-shaped flake of aggregate 0.6 in. long. This is the largest flake that remained in one piece after being scaled off by the salt. The aggregate this came from may also be seen in Figures 2, 10, 11, and 12.

about 1/16-in. thick and includes the surface of a limestone aggregate particle.

Figure 9 shows the surface of a cup after 12 salt cycles. The paste phase has scaled or flaked away and the coarse aggregate stands out in relief. The coarse aggregates shown in this photograph did not scale as much as the paste, but other aggregates do scale as seen in Figures 5, 6, and 8. All this was from salt scaling without any freeze-thaw. The cups and salt water were kept at ambient laboratory temperature of 68 to 74°F.

Many of the aggregates that scaled did so at their perimeter, adjacent to the zone of salt water movement at the aggregate borders. Figure 10 is the same cup as in Figure 2, but the cup has been slightly rotated in a clockwise direction for the photograph of Figure 10. This picture was taken after the salt water was emptied from the cup, the salt deposits dissolved by immersion in fresh water, and the cup allowed to air dry. Note the two aggregates near the top of the cup, just to the left of the letter A. (Three letters were placed about 120

FIGURE 9 A concrete cup that has gone through 12 cycles. Here the aggregates were more durable; the cement paste has weathered away and the limestone aggregates stand out in relief.

FIGURE 10 The same cup as shown in Figure 2 but rotated clockwise slightly to show another area. Note the two limestone aggregates at the top and to the left of the letter A. This cup is air drying between salt water treatments.

degrees apart around the top of the cups for aid in cup identification and to help in orientation of pictures; this particular cup was labeled ABC.)

Figure 11 shows the same area of the cup in Figure 10 after several more cycles of salt water treatment, immersion wash, and air drying. Note the perimeter of the two aggregates at the top of the cup to the left of the A. Both aggregates have a rim that has separated from the aggregate. This type of rim eventually flakes away, leaving a depressed border zone in the aggregate. At the center of Figure 11 are two elongated limestone aggregate particles with their long axis nearly vertical in the cup wall. The smaller of the two, a bean-shaped aggregate, is the flake shown in Figure 8. Figure 12 is the same general shot as Figure 11 after the flake in Figure 8 had scaled off; the pencil points to the spot where the flake came from. Other aggregates in both Figures 11 and 12 also have rims separating from the aggregate proper. A similarly scaled rim can be seen in the top right corner of Figures 5 and 6. Many of the same aggregates shown in Figures 10, 11, and 12 may also be seen in the right half of Figure 2. The location of the salt deposits are visible in Figure 2. After 12 cycles, about 95 percent of the limestone aggregates in this cup had been scaled to some extent.

Figure 13 shows a limestone coarse aggregate where the entire rim has flaked away, leaving the aggregate depressed compared to the cement paste. This is the opposite of the condition shown in Figure 9, where the paste has flaked away and the aggregates stand out in relief. The salt attacks the most susceptible component of the concrete—sometimes the paste, sometimes the aggregates, sometimes both. No two concretes are alike, but salt is persistent in finding a weakness to attack.

FIGURE 11 The same cup as in Figure 10 after more salt treatments. The two aggregates noted in Figure 10 show distinct rims that have separated from the rest of the aggregate due to salt weathering. Note the bean-shaped aggregate near the middle of the photograph.

FIGURE 12 The same cup as in Figure 11 after more salt weathering cycles. The bean-shaped aggregate surface has scaled away. The pencil points to where it was. The fragment shown in Figure 8 came from this location.

FIGURE 13 A limestone coarse aggregate particle with the entire rim flaked away by salt weathering. This left the aggregate surface depressed relative to the surrounding cement paste. No freeze-thaw was involved. Contrast the aggregate pictured here with those in Figure 9, where the paste was "eaten away" by salt.

Sometimes the salt water found preexisting cracks in the limestone aggregate particles. Figure 14 shows such a particle with salt deposits along cracks in the aggregate. Under freeze-thaw conditions this aggregate would probably have deteriorated from water freezing in the cracks.

One cup that went through several cycles of treatment began developing a rust deposit on the face of a limestone aggregate particle during the sixth cycle. This corrosion continued and ran down the inside face of the cup. The authors do not yet know what mineral in the aggregate is corroding, but they presume it is an iron oxide or an iron sulfide. Corrosion of minerals in the aggregates is another effect of salt weathering.

Three cups were treated internally with an alkyl-alkoxy silane type "sealer" such as used in the NCHRP 244 studies (*25*). This sealer did not prevent salt water movement through the limestone aggregates (*19*). One surprising result, however, was the cracking of all three silane-treated cups during the first cycle of salt water treatment. None of the nonsealed cups cracked even after as many as 12 cycles. Figure 15 shows one of the silane-treated cups with a pattern of cracks that goes through some limestone aggregates but alongside others. These were not the aggregates that the salt water passed through. Halite crystals at the top of the cup were deposited from evaporating salt water that wicked up the inside walls of the cup.

SUMMARY AND CONCLUSIONS

Many "clinical observations" made by KsDOT research geologists, as well as laboratory and field investigations, have provided information on how deicing salt (NaCl) weathers concrete and the aggregate in it. Salt exacerbates the alkali-aggregate reaction, D-cracking problem, and pavement blowup problem by keeping the concrete interior wet for longer periods of time. When the concrete and limestone aggregates remain wet, the dwell time of salt solution in the aggregates increases. This allows more time for other reactions to occur.

Degraded illite altered to sodium montmorillonite in limestone aggregate in Kansas bridge deck concrete. Sodium from

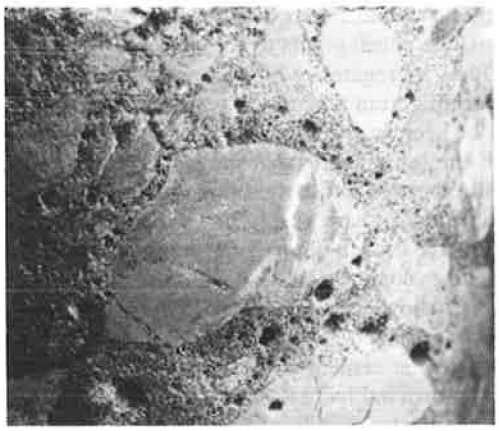

FIGURE 14 A limestone aggregate with preexisting cracks that salt water has moved through. This aggregate would probably deteriorate under freeze-thaw conditions.

FIGURE 15 Cracks in a silane "sealed" concrete cup that occurred during the first cycle of salt water treatment. The silane did not keep salt water from moving through many limestone aggregates. The cracks go through some aggregates and alongside others.

the deicing salt exchanged for potassium in the illite. The potassium, coupled with sodium and sulfate from the deicing salt, deposited as the mineral aphthitalite along with thernardite.

Salt scaling of concrete surfaces without freeze-thaw has been observed from outdoor exposure of concrete blocks. The use of concrete cups to monitor salt water (NaCl) movement through concrete helped to verify that deicing salt water can scale both the paste phase and the limestone aggregates without any freeze-thaw cycling. This is contrary to the claims of many that sodium chloride does not harm unreinforced concrete, aside from aiding and abetting freeze-thaw damage. The salt gradually corrodes or "gnaws away" at the cement paste and limestone aggregates, attacking the most accessible and susceptible portions first.

A silane sealer did not prevent salt water from moving through the limestone aggregates. All three cups treated on the inside with silane cracked on the first salt treatment cycle.

ACKNOWLEDGMENTS

Much of the early exploratory and development work for this study was conducted in cooperation with the Federal Highway Administration under the HP&R Program. FHWA's cooperation and especially their understanding of the possible importance of such exploratory studies are greatly appreciated. It is the authors' opinion that the FHWA Region 7 and Kansas Division's broad interpretation and flexibility in allowing exploratory work under the "Implementation of Research and Development" line item in the Annual Work Program has contributed as much to successful research in Kansas as any other single factor. They thank FHWA and KsDOT research administrators at all levels for their wise and flexible allowance of research charges. The payoff has been high (*27,28*).

The photographs used in this report were taken by engineering technicians Condie Erwin, John Knickerbocker, and Jeff Clarke while they worked with the project. Raymond K. Moore of the University of Kansas and others associated with the Kansas University Transportation Center provided copies of several papers used for review and references in this study. Their help is greatly appreciated, as is that of all others who contributed to the study and the processing of the manuscript.

REFERENCES

1. S. H. Kosmatka and W. C. Panarese. *Design and Control of Concrete Mixtures*, 13th ed. Portland Cement Association, Skokie, Ill., 1988, 205 pages.
2. G. G. Litvan. Phase Transition of Adsorbates: VI, Effect of Deicing Agents on the Freezing of Cement Paste. *Journal of the American Ceramic Society*, Vol. 58, No. 1–2, Jan.–Feb. 1975, pp. 26–30.
3. L. Dolar-Mantuani. *Handbook of Concrete Aggregates: A Petrographic and Technological Evaluation*. Noyes Publications, Park Ridge, N.J., 1983, 345 pages.
4. L. Dolar-Mantuani. Concrete Aggregate Examination by Prolonged Copper Nitrate Staining Method. *Ontario Hydro Research News*, Vol. 14, No. 2, 1962, pp. 4–14.
5. C. F. Crumpton and J. E. Bukovatz. Map Cracking in Limestone Sweetened Concrete Pavement Promotes D-Cracking. In *Transportation Research Record 651*, TRB, National Research Council, Washington, D.C., 1977, pp. 29–31.
6. P. P. Hudec and S. G. Rigby. The Effect of Sodium Chloride on Water Sorption Characteristics of Rock Aggregate. *Bulletin of the Association of Engineering Geologists*, Vol. XIII, No. 3, 1976, pp. 199–211.
7. R. E. Bisque and J. Lemish. Chemical Characteristics of Some Carbonate Aggregates as Related to Durability of Concrete. *Bulletin 196*, HRB, National Research Council, Washington, D.C., 1958, pp. 29–45.
8. R. E. Bisque and J. Lemish. Silicification of Carbonate Aggregates in Concrete. *Bulletin 239*, HRB, National Research Council, Washington, D.C., 1960, pp. 41–55.
9. H. D. Pflug and C. F. Crumpton. Chemische Verwitterungsvorgange im Beton. *Das Baugewerbe*, No. 7, April 1964, pp. 473–485 (German with English summary).
10. J. E. Bukovatz, C. F. Crumpton, and H. E. Worley. *Bridge Deck Deterioration Study, Final Report*. KsDOT and FHWA, Topeka, Kans., 1973, 44 pages.
11. H. D. Pflug and C. F. Crumpton. Analysis of Sodium in Concrete by Fluorescence Photometry. *Materials Research & Standards*, Vol. 3, No. 7, July 1963, pp. 556–560.
12. J. E. Bukovatz. *Bridge Deck Deterioration Study, Part 4—Field Exposure of Concrete Specimens. State Highway Commission of Kansas* (now KsDOT) and Federal Highway Administration, Topeka, Kans., 1969, 25 pages.
13. J. E. Bukovatz. *Bridge Deck Deterioration Study, Part 7—Weathering Test of Reinforced Concrete Slab with Various Depths of Steel*. State Highway Commission of Kansas (now KsDOT) and Federal Highway Administration, Topeka, Kans., 1968, 20 pages.
14. G. L. Morrison, Y. P. Virmani, F. W. Stratton, and W. J. Gilliland. *Chloride Removal and Monomer Impregnation of Bridge Deck Concrete by Electro-Osmosis*. Interim Report FHWA-KS-RD 74-1. Kansas Department of Transportation and Federal Highway Administration, Topeka, Kans., 1976, 38 pages.
15. G. P. Jayaprakash, J. E. Bukovatz, K. Ramamurti, and W. J. Gilliland. *Electro-Osmotic Techniques for Removal of Chloride from Concrete and for Emplacement of Concrete Sealants*. Report FHWA-KS-82-2. Kansas Department of Transportation and Federal Highway Administration, Topeka, Kans., Aug. 1982, 60 pages.
16. B. F. McCollom. Design and Construction of Conventional Bridge Decks that are Resistant to Spalling. *Transportation Research*

Record 604, TRB, National Research Council, Washington, D.C., 1976, pp. 1–5.
17. C. F. Crumpton and G. P. Jayaprakash. Salty Concrete Cups. *TR News*, No. 130, TRB, National Research Council, Washington, D.C., May–June 1987, p. 23.
18. C. F. Crumpton and G. P. Jayaprakash. Salt Water Readily Flows Through Fine Cracks in Concrete. *Concrete Construction*, Sept. 1987, p. 798.
19. C. F. Crumpton. Concrete 'Sealers' Fail in Salt Cup Tests. *Western Builder*, Sept. 3, 1987, pp. 40 and 42.
20. C. F. Crumpton and G. P. Jayaprakash. Invasive Salt Tough Foe, Study Finds. *Roads and Bridges*, June 1987, pp. 68 and 70.
21. C. F. Crumpton and G. P. Jayaprakash. Scanning Rust Crystals and Salt Crystals with Electron Microscope. *Transportation Research Record 860*, TRB, National Research Council, Washington, D.C., 1982, pp. 44–53.
22. C. F. Crumpton. Concrete—A Faithful Servant. *TR News*, No. 118, TRB, National Research Council, Washington, D.C., May–June 1985, pp. 3–7.
23. K. Ramamurti and G. P. Jayaprakash. Flocculation Modification to the Method of Determining Chloride in Portland Cement Concrete Powder. *Analyst*, Vol. 13, March 1988, pp. 523–524.
24. G. L. Morrison, Y. P. Virmani, K. Ramamurti, and W. J. Gilliland. *Rapid In-Situ Determination of Chloride Ion in Portland Cement Concrete Bridge Decks*. Report FHWA-KS-RD-75-2. KsDOT and FHWA, Topeka, Kans., Nov. 1976, 35 pages.
25. D. W. Pfeifer and M. J. Scali. *NCHRP Report 244: Concrete Sealers for Protection of Bridge Structures*. TRB, National Research Council, Washington, D.C., 1981, 138 pages.
26. M. O. Withey. Soundness Tests for Coarse Aggregates. *HRB Proc.*, Vol. 4, 1924, pp. 109–111.
27. C. F. Crumpton. Another Day—Another $20,000 of Savings Realized from Kansas DOT Research and Development Studies. *TR News*, No. 122, TRB, National Research Council, Washington, D.C., Jan.–Feb. 1986, pp. 11–14.
28. KDOT Research Efforts Save $20,500—Per Day. *KUTC Newsletter* (University of Kansas Transportation Center), Vol. 9, No. 2, May 1987, pp. 1 and 10.

Evaluation of Carbonate Aggregate Using X-Ray Analysis

WENDELL DUBBERKE AND VERNON J. MARKS

Iowa has more than 13,000 miles of portland cement concrete (PCC) pavement. Some pavements have performed well for over 50 years, while others have been removed or overlaid due to the premature deterioration of joints and cracks. Some ot the premature deterioration is classical D-cracking, which is attributed to a critically saturated aggregate pore system (freeze-thaw damage). However, some of the premature deterioration is related to adverse chemical reactivity involving carbonate coarse aggregate. The objective of this paper is to demonstrate the value of a chemical analysis of carbonate aggregate using X-ray equipment to identify good or poor quality. At least 1.5 percent dolomite is necessary in a carbonate aggregate to produce a discernible dolomite peak. The shift of the maximum-intensity X-ray diffraction dolomite d-spacing can be used to predict poor performance of a carbonate aggregate in PCC. A limestone aggregate with a low percentage of strontium (less than 0.013) and phosphorus (less than 0.010) would be expected to give good performance in PCC pavement. Poor performance in PCC pavement is expected from limestone aggregates with higher percentages (above 0.050) of strontium.

Over 13,000 miles of Iowa's 35,000 miles of paved highways are portland cement concrete (PCC). Many of the 22,000 miles of asphalt concrete pavement were originally PCC pavement that has been overlaid. The extent of the maintenance-free life of these PCC pavements is very dependent on the quality of coarse aggregate used. Some PCC pavements have performed well for over 50 years, while others have failed prematurely. The premature failures are predominantly deterioration of joints and cracks (Figure 1). This deterioration is generally referred to as D-cracking. In a recent synthesis (*1*), D-cracking is defined as "a form of PCC deterioration associated primarily with the use of coarse aggregates in the concrete that disintegrate when they become saturated and are subjected to repetitive cycles of freezing and thawing."

Iowa research in the 1960s identified many crushed stone aggregate sources that would, in a saturated condition, cause rapid deterioration of PCC due to freezing and thawing. Initial testing and identification was based on ASTM C666, Method B. Research beginning in 1978 established a relationship between the freeze-thaw failure of carbonate aggregates and their pore systems (*2,3*).

Within the last 10 years, poor performance of many miles of PCC pavement has been determined to be related to the use of carbonate aggregates with open, large pore systems not prone to critical saturation and subsequent freeze-thaw disintegration. These aggregates cause adverse chemical reactivity, resulting in pavement deterioration visibly similar to D-cracking. The amount or rate of deterioration is directly related to the amount of deicing salt used on the pavement (*4*). This finding suggests that there are at least two types of rapid joint deterioration: the classical D-cracking failure as defined in the recent synthesis (*1*), and another type that can be related to the trace elements in the carbonate aggregate. The trace elements contribute to chemical reactions that alter and weaken the crystalline structure of the carbonate aggregate and the cement paste.

High-quality aggregates are essential to durable concrete. Iowa is using the Mercury Porosimeter and the Iowa Pore Index Test to identify carbonate aggregates with pore systems that are susceptible to rapid freeze-thaw deterioration. Previous Iowa research (*5*) has shown that aggregates that exhibit a predominance of pore sizes in the 0.04- to 0.2-micron diameter range are susceptible to critical saturation and subsequent freeze-thaw deterioration. Generally, aggregates that do not contain a predominance of these pore sizes are not prone to freeze-thaw (D-cracking) deterioration. Similar deterioration of some PCC pavements made using coarse aggregates with pore sizes larger than 0.2 micron in diameter prompted the research on premature failure associated with chemical reaction.

OBJECTIVE

The objective of this research was to demonstrate the value of chemical analyses using X-ray equipment to identify good or poor carbonate aggregate quality.

GEOLOGIC IDENTIFICATION OF IOWA CARBONATES

Beginning in the 1940s, Iowa geologists began developing geologic sections for quarries producing crushed carbonates for use in Iowa. The geologic sections describe the beds in all the ledges that are or at one time were approved for use in PCC pavement. These sections show the correlation of all concrete ledges with the geologic column for Iowa. Final acceptance of coarse aggregate for PCC pavement is based on quality testing of the aggregate produced.

Pavement history records, which include the quarry ledges by bed used to produce the coarse aggregate, have been maintained since 1940. Iowa geologists continually inspect pavements and record when visible deterioration of joints due to the aggregate is identified. A service record of years to visible deterioration is thereby developed for all the ledges of stone used in Iowa PCC pavement.

Iowa Department of Transportation, Ames, Iowa 50010.

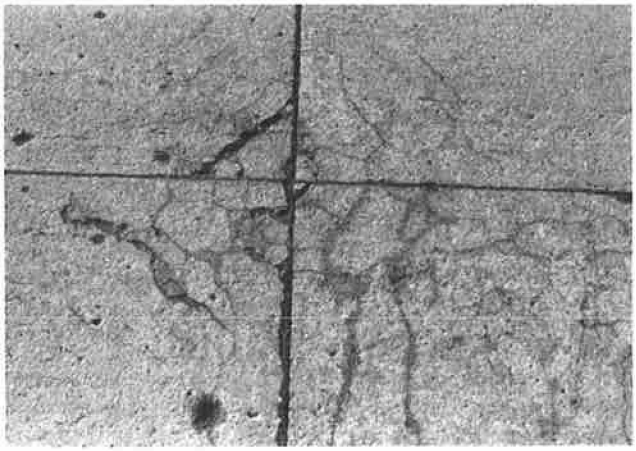

FIGURE 1 Close-up of premature deterioration at an intersection of the transverse and longitudinal joints.

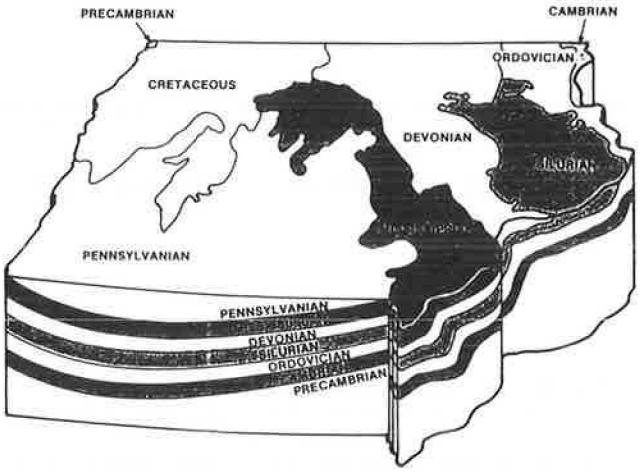

FIGURE 2 A stratigraphic cross-sectional view of Iowa geologic systems.

Approximately 75 percent of the coarse aggregate used in Iowa PCC pavement is crushed carbonate. The other 25 percent is river gravel containing 20 to 70 percent carbonate particles. Geologically, the Paleozoic strata of Iowa are part of the Forest City Basin, which extends into Missouri, Kansas, and Nebraska (*6*). A cross-sectional view of the stratigraphic system is shown in Figure 2. With the exception of a small amount of sandstone and a very small area of gypsum the quarried bedrock is carbonate. The Pennsylvanian System generally yields poor quality stone. The Mississippian, Devonian, and Ordovician systems contain units that yield carbonate aggregates of poor to good quality. The best aggregates are obtained from the Silurian System.

X-RAY EQUIPMENT

The X-ray equipment used for elemental analysis of the carbonate aggregate is located at Iowa State University (ISU) (*7*). The ISU facilities include two scanning electron microscopes (SEMs), a sequential X-ray spectrometer, and an X-ray diffractometer. Since 1980, a software package providing automated image analysis has been added, thereby expanding the capabilities of the SEMs.

Electron microscopes scan across a specimen using a highly focused beam of electrons. When the beam strikes the surface of the sample, X-rays and secondary electrons are emitted. A positively charged detector attracts the negatively charged electrons and converts them into an electric current. An image of the sample is then displayed on a cathode ray tube. The newly obtained JEOL JSM-840A scanning electron microscope allows for easier operation and for observations with higher resolution of ultramicro surface structures than the JEOL JSM-U3, which was purchased in 1971. Both SEMs are equipped with an energy dispersive X-ray analyzer, which can identify elements present in the sample by the X rays they emit when the electron beam strikes them.

The SRS-200 automated sequential X-ray spectrometer analyzes elements by fluorescence. The spectrometer excites the samples using X rays and, by measuring the X rays emitted from the sample, elemental concentrations can be determined. The SRS-200 is capable of analyzing 10 samples at a time for up to 30 elements.

Using the Siemens D500 X-ray diffractometer, analysis of compounds is performed through the determination of spacings of crystallographic planes by diffraction of X rays. The D500/SRS-200 system uses two microcomputers for its analytical operations. The data can also be transmitted to the ISU mainframe computer for further evaluation.

SAMPLE SIZE AND PREPARATION

The new JEOL JSM-840A SEM will accommodate samples up to 4 in. in diameter and ½-in. thick. For initial evaluation, a broken piece with a relatively flat plane can be used without further preparation. A quick elemental analysis can be conducted to determine if further analysis is warranted. This also gives direction as to what elements should be selected for final analysis. Photographs are taken at relatively low voltage. Good-quality photographs can sometimes be taken without a special coating, but normally a gold, carbon, or silver coating is applied to prevent an electrical charge from occurring and interfering with the photograph. For final chemical analysis, the area of interest must be flat and polished. Rapid sawing with a diamond blade had been used to obtain a smooth flat face. This procedure is no longer used because it heats igneous and other hard particles and causes damage to the surface. Slow sawing with a lapidary diamond blade does not overheat the hard particles.

For X-ray fluorescence (XRF), the material to be analyzed is crushed for 2 min in a Spex Shatterbox (ring grinder) to produce material passing the Number 300 sieve. If a mechanical mixture is being prepared, care should be taken to try to obtain uniform particle size. Silica is a problem when crushed with the softer carbonate material. Grinding a mixture of harder and softer particles produces nonuniform particle sizes that do not allow for precise quantitative analysis. An extended period of grinding alleviates this problem. The sample holder is a 1-in.-diameter plastic cylinder. A plastic ring is used to attach a sheet of 6-micron-thick mylar to the bottom, making a cup. A ¼-in. layer of loose crushed dolomite or limestone

is poured into the cup. The top of the sample is covered with a sheet of 6-micron-thick mylar and fastened with another plastic ring.

The sample for X-ray diffraction (XRD) is crushed to the same size as for XRF. When the determination of a very exact d-spacing or a minor shift in a d-spacing is desired, approximately 10 percent crushed zirconia is mixed with the carbonate sample as a standard reference. Enough powdered sample material is placed in a 1-in.-diameter, 1/16-in.-deep plastic cup to overfill the cup. A strike off is used to remove excess material.

COMPOSITION OF AGGREGATE

There are times when the composition of an aggregate is an important factor in ascertaining its quality. Laboratory testing of the igneous fraction of Iowa river gravels always yields good performance in PCC. In some areas of Iowa, the carbonate fraction (up to 70 percent) of a river gravel produces premature failure in PCC pavement. In the past, it took an experienced petrographer to manually separate the various rock types.

With XRD, there is a much quicker, more accurate, and less labor-intensive method of conducting a petrographic analysis. The material to be analyzed is first crushed to pass the Number 4 sieve. This material is then split to yield a uniform representative sample. This representative sample is then ground in the Spex Shatterbox as previously explained. A software package has been obtained by ISU that will graphically display the percentage of each of the different rock types. Petrographic analysis of river sands is now being conducted. A sample of the computer output is shown in Figure 3.

A program to systematically determine the elemental analysis of Iowa carbonates began five years ago. During that time, percentages of various elements have been determined on over 1,700 samples. Some elements (Na and Cl) have shown no relationship to aggregate performance and are no longer included. The Iowa Department of Transportation (DOT) has recognized the benefits of using X-ray analysis of carbonate aggregate in determining quality of coarse aggregate for use in PCC pavement. Some carbonates from other states, generally exhibiting poor performance, have been included in the X-ray analysis program. The X-ray analyses of this limited number (57 samples) do not conflict with the findings for Iowa carbonates.

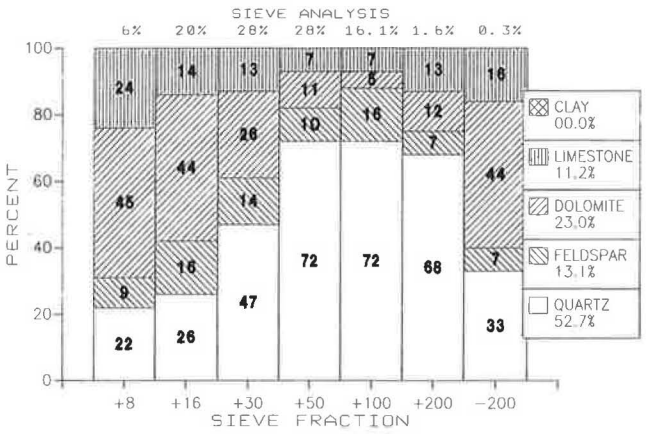

FIGURE 3 XRD petrographic analysis of river sand.

Because the research is being conducted on dolomites, $CaMg(CO_3)_2$, and limestones, $CaCO_3$, many of the elements are almost entirely contained as one compound. For instance, the calcium is almost entirely combined as $CaCO_3$ or limestone. Almost all of the magnesium would be in the form of $CaMg(CO_3)_2$ or dolomite. All of the X-ray chemical analyses for this research have been by XRF for elements, with an assumption as to the compounds. The percentages of calcium and magnesium provide information to determine the ratio of limestone to dolomite. XRD peak intensities can also provide this ratio information. Current research with XRD verifies the validity of the limestone-dolomite relationship determined using XRF elemental analysis.

Analysis by XRF yields the percentages of elements present in a sample. Prior to X-ray analysis the percentage of strontium found in a sample was usually expressed as strontium oxide. The authors do not believe that these elements are contained in the carbonates as oxides and, therefore, will not express them in that manner. All percentages expressed in this paper will refer to elemental strontium and elemental phosphorus. The conversion factor that may be used to determine how much strontium oxide this would represent is 1.1826. The conversion factor from elemental phosphorous to phosphorous oxide is 2.2913.

Currently the Iowa DOT uses a 16-cycle, water-alcohol freeze-thaw test (FTA) with a specified loss of not more than 6 percent of the total sample weight for acceptance of coarse aggregate for PCC. The percentage loss is directly related to the amount of clay in the carbonate. Most of the elemental aluminum and titanium are contained in clays and, therefore, they correlate with the results of the water-alcohol freeze-thaw test (Figures 4 and 5). Two factors that hinder this correlation are the presence of authigenic feldspar containing aluminum and titanium and the use of different gradations of aggregate in the freeze-thaw test. When the same gradation is used for the freeze-thaw test and the aggregate is from the same quarry (Festina), a high correlation ($r = 0.93$) is obtained (Figure 6). The correlation coefficient of elements (for 86 samples) with each other and with water-alcohol freeze-thaw is given in Table 1. Aluminum ($r = 0.65$) and titanium ($r = 0.62$) show the greatest correlation with the FTA. The elemental analysis of a few carbonates selected to give a range of limestone and dolomite aggregates from good to poor performance is given in Table 2.

The SEM is used to examine limestones, dolomites, and PCC. A deteriorated dolomite aggregate in PCC exhibited a dark rim (Figure 7). An initial assumption was that the rim would be high in iron. A SEM spot analysis showed no iron but a high sulfur, calcium, and silicon content. An investigation of the dark rim is continuing. Speculation is that a chemical reaction has occurred at the boundary of the dolomite particle, which adversely affects the bond.

EVALUATION OF DOLOMITIC AGGREGATE

XRD has become the principal Iowa method of identifying dolomitic aggregate that will result in poor performance in

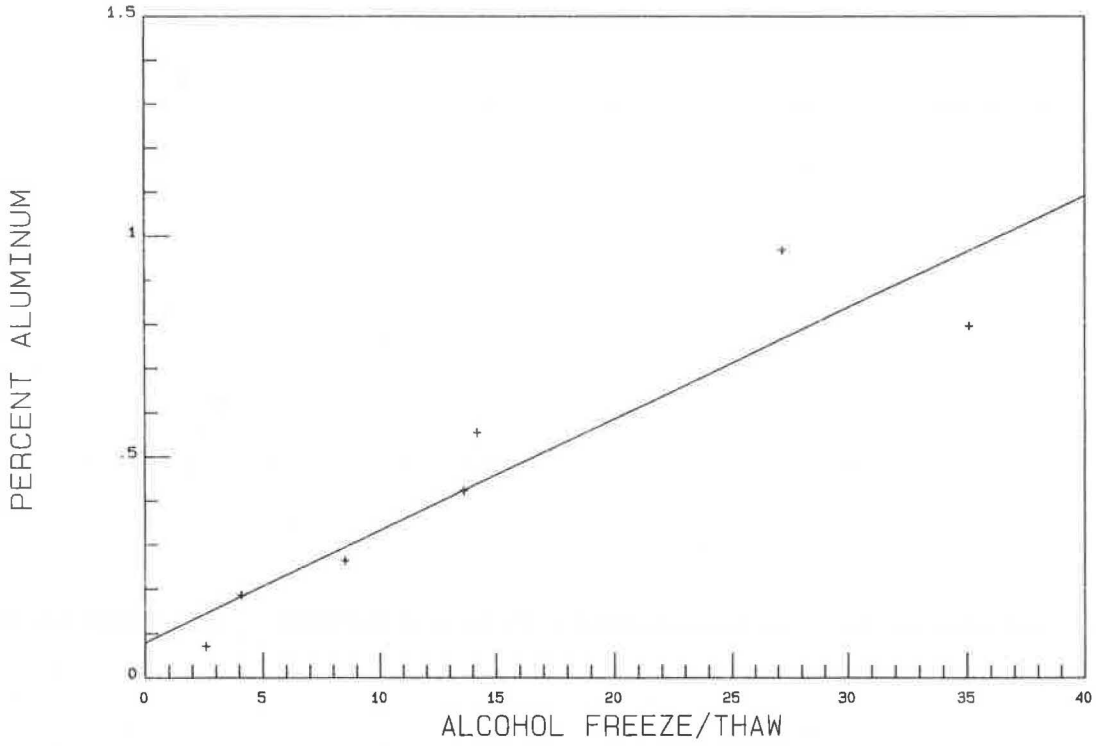

FIGURE 4 Alcohol freeze-thaw versus percent aluminum.

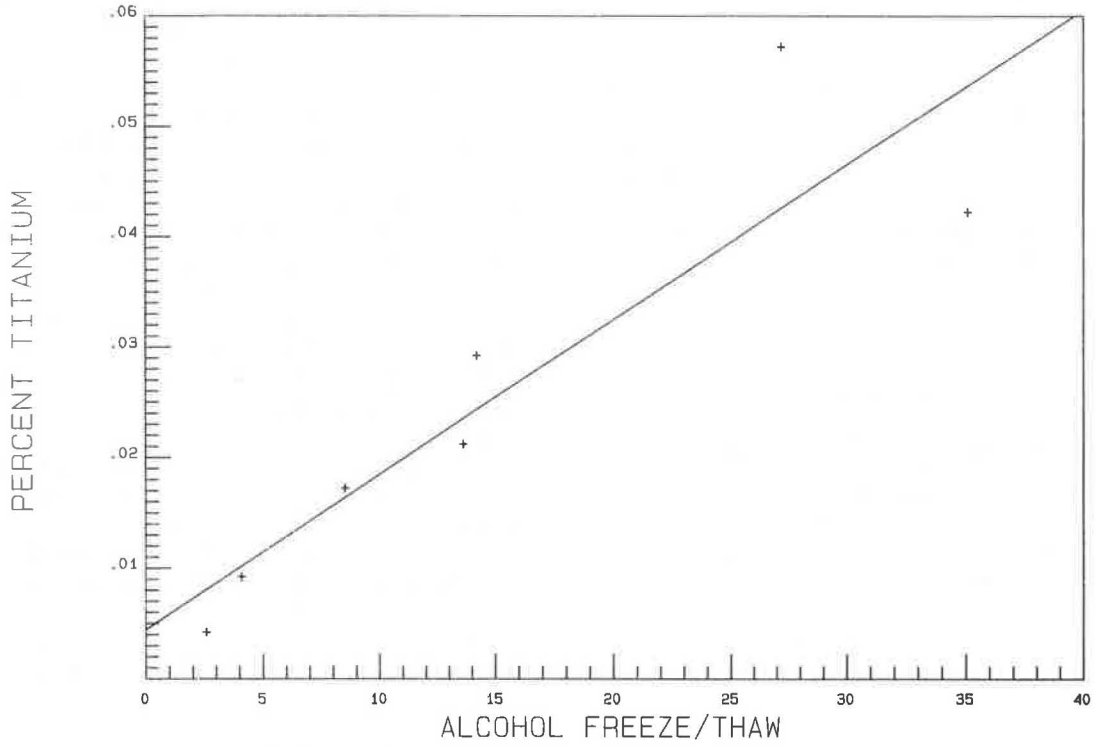

FIGURE 5 Alcohol freeze-thaw versus percent titanium.

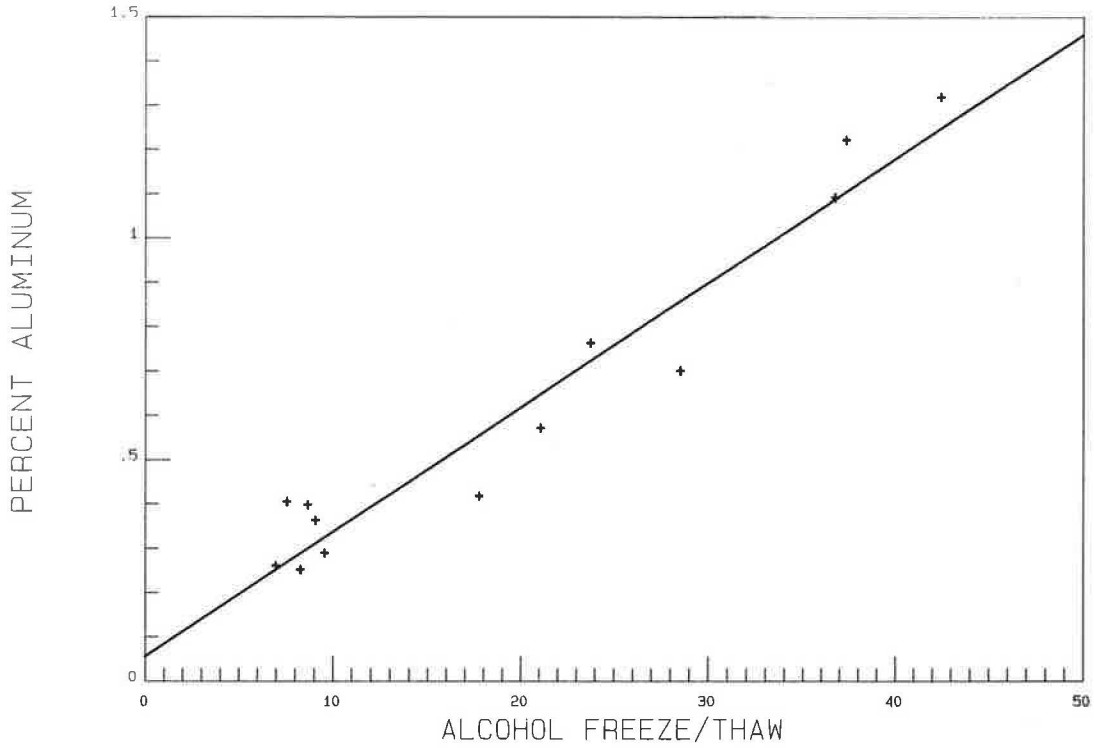

FIGURE 6 Alcohol freeze-thaw versus percent aluminum for the Festina Quarry.

TABLE 1 A SUMMARY OF CORRELATION COEFFICIENTS FOR ELEMENTS IN CARBONATES AND THE WATER-ALCOHOL FREEZE-THAW

	Sr	Mg	Fe	S	Ti	Mn	Si	Ca	K	P	Al
Mg	-0.30	1.00									
Fe	0.27	-0.05	1.00								
S	0.01	0.00	0.09	1.00							
Ti	0.34	-0.12	0.63	0.08	1.00						
Mn	0.10	0.05	0.32	0.04	0.16	1.00					
Si	0.21	-0.19	0.48	0.00	0.55	0.17	1.00				
Ca	0.07	-0.56	-0.41	-0.16	-0.36	-0.16	-0.54	1.00			
K	0.21	-0.11	0.33	-0.00	0.43	0.06	0.52	-0.44	1.00		
P	0.43	-0.24	0.44	0.00	0.58	0.11	0.34	-0.11	0.32	1.00	
Al	0.41	-0.21	0.59	0.03	0.73	0.21	0.80	-0.47	0.68	0.50	1.00
FTA	-0.08	-0.07	0.30	0.23	0.62	-0.10	0.60	-0.10	0.61	0.35	0.65

PCC pavement. In a stone consisting of a mixture of limestone and dolomite, at least 1.5 percent dolomite is needed to yield a discernible dolomite peak. If a discernible dolomite peak can be identified, poor performance in PCC pavement can be predicted by the maximum-intensity X-ray diffraction dolomite d-spacing (XRD d-s) (*4*). A high maximum-intensity dolomite-ankerite d-spacing (greater than 2.899) would identify a carbonate with poor performance in PCC pavement (Figure 8).

The pore system of the aggregate significantly affects the rate of adverse chemical reactivity. At this time, the relationship of the pore size effect on chemical reactivity has not been fully determined. This relationship is not intended to show that 1.5 percent poor-quality dolomite can cause rapid

TABLE 2 XRF ELEMENTAL ANALYSES OF A RANGE OF CARBONATES

Quarry	SR	XRD d-S	PERCENTAGES Sr	Mg	Ca	Al	Fe	S	Ti	Si	P
Maryville	40	2.889	0.010	12.66	21.78	0.13	0.16	0.02	0.01	0.44	0.00
Aurora	40	2.887	0.011	11.72	22.51	0.17	0.19	0.02	0.01	1.04	0.00
Pape	30	None	0.011	0.22	38.32	0.28	0.12	0.04	0.01	1.22	0.00
Daley	30	2.887	0.008	12.59	21.36	0.22	0.58	0.07	----	0.63	----
Gil City	30	None	0.016	0.23	38.33	0.30	0.21	0.13	0.01	1.05	0.00
Kendall-ville	25	2.889	0.015	6.41	28.72	0.37	0.55	0.38	0.02	1.69	0.02
Skyline	25	2.891	0.024	3.42	30.84	0.58	0.43	0.19	0.03	3.87	0.03
Weeping Water	25	None	0.041	0.23	39.11	0.08	0.18	0.08	0.00	0.44	0.01
LeGrand	20	2.902	0.014	8.02	27.84	0.12	0.83	0.17	0.01	0.38	0.03
Smith	15	2.901	----	10.89	23.83	0.15	0.49	0.17	0.01	0.62	0.01
Logan	15	2.902	0.054	0.76	35.33	0.53	0.54	0.19	0.03	3.13	0.03
Garrison	15	2.904	0.021	10.67	23.53	0.16	1.06	0.65	0.01	0.71	0.01
Glory Rapid	10	2.903	0.016	9.86	19.40	1.48	1.05	0.43	----	5.47	----
Kingston, ONT	10	2.908	0.038	5.21	24.94	1.98	1.04	0.23	0.11	5.96	0.01
Ullin, IL	10	2.890	0.259	1.15	35.83	0.18	0.17	0.37	0.01	2.34	0.05
VA	?	2.903	0.033	1.34	36.36	0.35	0.39	0.19	0.02	1.34	0.01
Tyrone, KY	?	2.904	0.032	2.76	32.09	0.86	0.50	0.16	0.04	3.20	0.13
Jefferson	5	2.906	0.068	0.46	37.55	0.20	0.29	0.04	0.01	1.66	0.02
Stanzel	5	2.907	0.055	0.43	38.30	0.14	0.47	0.06	0.01	0.79	0.01
Ada, OK	?	2.908	0.017	0.18	38.16	0.22	0.28	0.10	0.01	0.74	0.54
C. Hill, TN	?	None	0.055	0.41	38.64	0.16	0.15	0.14	0.01	0.53	0.05

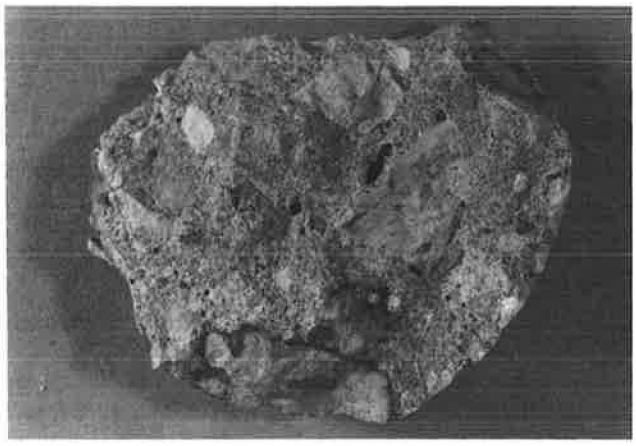

FIGURE 7 PCC containing a deteriorated dolomite aggregate with a dark rim.

deterioration of PCC pavement. Speculation is that the detrimental element, compound, or characteristic is also present in the limestone fraction of the carbonate particle.

X-ray analyses of over 120 samples have shown very low amounts (less than 0.025 percent) of strontium in dolomite aggregates.

EVALUATION OF LIMESTONE AGGREGATE

X-ray analyses have yielded data that will generally predict good or bad performance of limestone ($CaCO_3$) aggregate in PCC pavement. A good correlation for the full range has not been identified. There is a very small d-spacing shift of the maximum-intensity limestone ($CaCO_3$) peak as compared to the large d-spacing shift for dolomites. Zirconia was added to the carbonate sample to improve accuracy in the analysis

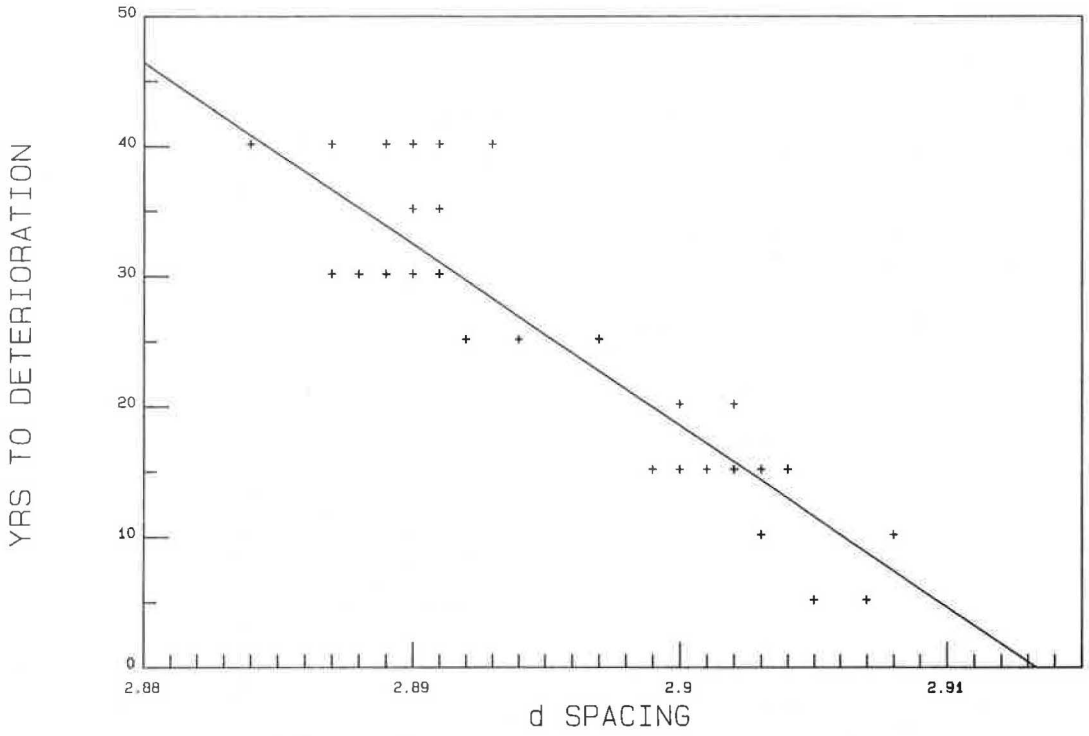

FIGURE 8 Graph of d-spacing of maximum-intensity dolomite peak versus years to visible deterioration of the concrete.

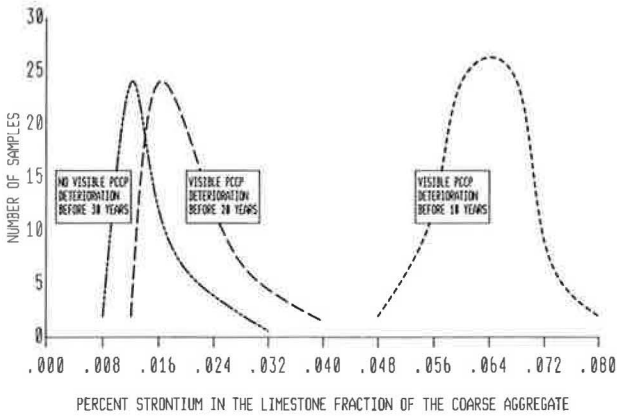

FIGURE 9 Relationship of percent strontium in the carbonate aggregate to service record when used in PCC pavement.

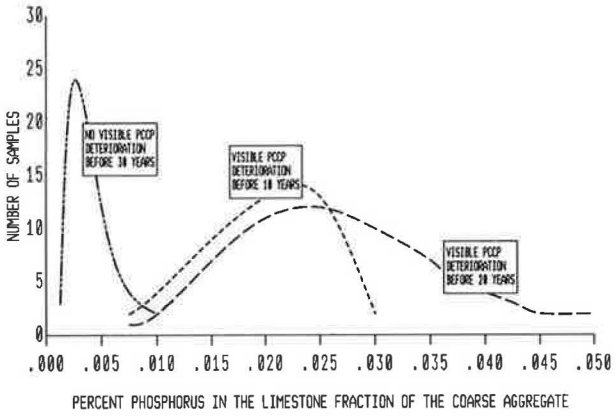

FIGURE 10 Relationship of percent phosphorus in the carbonate aggregate to service record when used in PCC pavement.

of peak shifts. Research to date has not shown a good correlation of this shift with limestone (calcite) performance records.

Strontium, an element not found in significant amounts in dolomite aggregates tested by the Iowa DOT, relates to performance of limestone aggregate in PCC pavement. Phosphorus is another element that exhibits a relationship to the performance of limestone aggregate in PCC pavement. If a limestone aggregate is low in strontium (below 0.013 percent) in the limestone fraction of the carbonate particle (Figure 9) and low in phosphorus (below 0.010 percent) in the limestone fraction (Figure 10), good performance in PCC pavement is expected. Poor performance is expected if the strontium in the limestone fraction of the aggregate exceeds 0.050 percent. Iowa limestones from the Silurian System (less than 0.013 percent strontium) exhibit the best performance, while Pennsylvanian limestones (generally above 0.040 percent strontium) exhibit the poorest performance. Within the Pennsylvanian System, the Stanzel Quarry has the poorest performance and the highest percent strontium (0.055), while the Weeping Water Quarry has the best performance and the lowest percent strontium (0.041). The service record in years to visible deterioration of PCC pavement shows a correlation coefficient of $r = -0.38$ with strontium (for 367 samples), $r = -0.22$ with phosphorus (for 376 samples), and $r = -0.40$ with strontium plus phosphorus (for 367 samples).

CONCLUSIONS

This research on X-ray analysis of carbonate aggregates supports the following conclusions:

1. X-ray analysis of Iowa carbonate aggregates is an effective method of predicting their performance in PCC pavement.
2. For Iowa carbonate aggregates with more than 1.5 percent dolomite, the maximum-intensity X-ray diffraction dolomite d-spacing can be used to predict poor performance in PCC concrete.
3. Iowa limestone aggregates with large, open pore systems, strontium below 0.013 percent, and phosphorus below 0.010 percent exhibit good performance in PCC pavement.
4. Iowa limestone aggregates with strontium above 0.050 percent will exhibit poor performance when used in PCC pavement.

ACKNOWLEDGMENTS

The authors wish to express their appreciation to Turgut Demirel, Jerry Amenson, Scott Schlorholtz, and Glen Oren of Iowa State University for their assistance in X-ray analysis of aggregates and in the interpretation of the data. The use of ISU equipment made the research possible. Jim Myers, Scott Graves, and Kathy Davis were very helpful in preparation of the report.

REFERENCES

1. D. Schwartz. *NCHRP Synthesis of Highway Practice 134*: D-Cracking of Concrete Pavements. TRB, National Research Council, Washington, D.C., October 1987.
2. J. Myers and W. Dubberke. *Iowa Pore Index Text*. Interim Report. Iowa Department of Transportation, Ames, Iowa, Jan. 1980.
3. W. Dubberke. Factors Relating to Aggregate Durability in Portland Cement Concrete. Interim Report HR-2022. Iowa Department of Transportation, Ames, Iowa, Jan. 1983.
4. W. Dubberke and V. Marks. The Relationship of Ferroan Dolomite Aggregate to Rapid Concrete Deterioration. *Transportation Research Record 1110*. TRB, National Research Council, Washington, D.C., 1987, pp. 1–10.
5. V. Marks and W. Dubberke. Durability of Concrete and the Iowa Pore Index Text. *Transportation Research Record 853*. TRB, National Research Council, Washington, D.C., 1982, pp. 25–30.
6. W. Anderson. *Geology of Iowa–Over Two Billion Years of Change*. The Iowa State University Press, Ames, Iowa, 1983.
7. J. Amenson and T. Demirel. *Materials Analysis and Research Laboratory: Capabilities, Engineering Research Institute*. Iowa State University, Ames, Iowa, September 1985.

Laboratory Evaluation of Shape and Surface Texture of Fine Aggregate for Asphalt Concrete

W. R. MEIER, JR., AND EDWARD J. ELNICKY

The evaluation of the shape and surface texture of various fine aggregates was studied. Asphalt concretes using these fine aggregates were evaluated for mix design and deformation under load. Seven different test procedures for evaluating aggregate shape and surface texture were studied. Three sources of fine aggregate with four percentages of crushed material were utilized for both the fine aggregate and the asphalt concrete studies. Of the seven tests for aggregate shape and surface texture, all but the direct shear test provided data that correlated with the percentage of fine aggregate with crushed faces. Best results were obtained from the National Crushed Stone Association (now the National Aggregates Association) test, the Rex and Peck time index, and the specific rugosity. These results were correlated to the Hveem stability of asphalt concrete mixtures designed to a constant 4 percent air voids using the study aggregates. Similar correlations were performed with Hveem stability and asphalt concrete mixtures with an additional 0.5 percent asphalt binder. Statistically significant relationships were found between the results of these aggregate tests and the Hveem stabilities.

The properties of asphalt concrete depend on a large number of factors, many of which relate to the aggregate used. It is recognized that the aggregate shape and surface texture have a significant effect on these properties. Whereas aggregate gradation and durability have fairly definitive tests, aggregate shape and surface texture generally do not. Visual examination of coarse aggregate particles larger than the No. 4 or No. 8 sieve is used to identify particles with fractured faces. This is the most common method of judging aggregate shape and surface texture. This method has a number of drawbacks; one is that it tells nothing about the fine aggregate.

Investigators have determined that the properties of the asphalt alone are not sufficient to predict or control the deformation of asphalt concrete mixtures. As early as 1954, Herrin and Goetz (*1*) reported on the effect of aggregate shape on stability of bituminous mixtures. In 1956, Rex and Peck (*2*) developed a simple direct test to measure the relative angularity and surface roughness of sand. Huang (*3*) developed a particle index test (rhombohedron mold) to reflect the discernible geometric characteristics of an aggregate. Tons and Goetz (*4*) measured specific rugosity and packing volume of aggregates. In 1977, Ishai and Tons (*5*) developed a pouring test for the direct measurement of the packing specific gravity of one-sized aggregate particles.

McLeod and Davidson (*6*) presented test data showing that 2- and 3-in. diameter molds could be used to determine the particle index values for fine aggregates. Other procedures, such as a 1959 test proposed by the National Crushed Stone Association (the National Crushed Stone Association is now the National Aggregates Association), have been used.

The geometric irregularity of aggregate particles has a major effect on the physical properties and mechanical behavior of bituminous paving mixtures. Griffith and Kallas (*7*) determined that the type of fine aggregate greatly influenced the stability of asphaltic mixtures. Boutilier (*8*) determined that there was a relationship between the particle index of an aggregate and the physical properties of a bituminous aggregate mixture. Further work of Ishai and Tons (*9*), Kalcheff and Tunnicliff (*10*), and Ishai and Gelber (*11*) has produced in-depth evidence that the surface texture of the aggregate is a significant factor in the deformation characteristics of bituminous mixtures.

This project was conducted to evaluate various test methods that provide information about the shape and surface texture of fine aggregate for asphalt concrete. It was also intended to relate these fine aggregate properties to asphalt concrete properties.

MATERIALS

Aggregates

Three aggregate sources were selected for use in the test program. Crushed basalt was obtained from Flagstaff, Arizona, and crushed river gravels were obtained from the Salt River in Phoenix, Arizona, and the Santa Cruz River near Tucson, Arizona. For reference throughout the study, these were referred to as Flagstaff, Salt River, and Tucson sources. Uncrushed fine aggregate was also obtained from the Santa Cruz River source at Tucson. Physical properties for coarse and fine aggregates are shown in Table 1.

Asphalt

AC-20 asphalt cement for the asphalt concrete testing came from the Edgington Refinery (Wilmington crude) source. Physical properties of the asphalt cement are shown in Table 2. A large number of samples of asphalt cement were taken in metal containers. The contents of a container were heated to mixing temperature when required for batching mixtures, and any unused material was discarded. This allowed all work

Western Technologies Inc., P.O. Box 21387, Phoenix, Ariz. 85036.

TABLE 1 PHYSICAL PROPERTIES OF AGGREGATES

Crushed Coarse Aggregate

	Salt River	Tucson	Flagstaff
L.A. Abrasion	20.5	15.7	14.4
Bulk Sp. Gr.	2.650	2.530	2.840
S.S.D. Sp. Gr.	2.673	2.571	2.865
App. Sp. Gr.	2.712	2.638	2.913
Absorption (%)	0.86	1.63	0.88

Crushed Fine Aggregate

	Salt River	Tucson	Flagstaff	Tucson(1)
Bulk Sp. Gr.	2.632	2.510	2.920	2.456
S.S.D. Sp. Gr.	2.664	2.561	2.946	2.519
App. Sp. Gr.	2.719	2.647	2.999	2.620
Absorption (%)	1.21	2.06	0.91	2.50
Sand Equivalent	82	73	41	81

(1) Uncrushed Fine Aggregate

TABLE 2 PHYSICAL PROPERTIES OF AC-20 ASPHALT CEMENT

Property	Unit	Test Value
Absolute Viscosity @ 140F	Poises	2235
Kinematic Viscosity @ 275F	cSt	263.1
Penetration @ 77F	1/10 mm	44
Flash Point, Cleveland Open Cup	F	529
Solubility in Trichloroethylene	Percent	99.98
Absolute Viscosity @ 140F (1)	Poises	4262
Ductility (1)	cm	50+

(1) Tests conducted on residue from thin film over test

to be performed using asphalt cement in a once-heated condition, so that the properties of the asphalt cement used would be constant.

Aggregate Preparation

The basalt aggregate obtained from Flagstaff had been crushed from a ledge source and contained all newly fractured faces. The Salt River and Tucson materials required laboratory crushing to obtain fine aggregate with fractured faces on all particles.

The crushed river gravels were dried, and the material passing the No. 4 sieve was discarded. The aggregate larger than the No. 4 sieve was put through a laboratory jaw crusher three to five times to produce a material with a maximum size of approximately ¼ in. During laboratory crushing, it was necessary to maintain a surcharge of material over the jaw opening to reduce the production of elongated particles.

Following crushing, the aggregates were separated into several fractional sizes, from the No. 4 sieve to the No. 200 sieve and passing the No. 200 sieve, by mechanically shaking the dry material. The Flagstaff fine aggregate and the uncrushed fine aggregate from the Tucson source were separated into sizes in a similar manner. Coarse aggregates from the three study sources were mechanically sieved into fractional sizes between ¾ in. and the No. 4 sieve. Aggregate gradation control during the study was accomplished by proportioning the individual fractions of aggregate.

TEST PROCEDURES

Tests of aggregate shape and surface texture and tests of asphalt concrete were performed during this study. A brief description of the tests follows.

Tests of Aggregate Shape and Surface Texture

National Crushed Stone Association

This test was used to determine the voids in individual fractions of fine aggregate. A cylinder of known volume was filled by letting aggregate flow into the cylinder in a standard manner until it was overflowing. The cylinder was then carefully

struck off and weighed. The sand was recombined, and two additional weight determinations were made. Three different-sized aggregate fractions were used, and an average test result of the three results was calculated.

Index of Aggregate Particle Shape and Texture

This test provided an index value of the relative particle shape and texture characteristics of aggregates. A single fraction of aggregate was compacted in a mold using two different compactive efforts (10 and 50 drops). The test was completed on six different aggregate fractions between the No. 4 and No. 200 sieves. An index value was obtained for each aggregate fraction. The weighted average index for the composite aggregate was obtained by using the proportions of each aggregate fraction and its index value.

The test procedure followed ASTM Method D3398-81 except for the mold and tamping rod used. A mold 3 in. in diameter, 3.5 in. in height, and 54 in.^{3} in volume was used. The tamping rod was 5/16 in. in diameter, approximately 12 in. long, and weighed between 0.254 and 0.259 lb.

Rex and Peck Time Index

This test was developed on the principle that smooth-textured, rounded sand particles offer less resistance to free flow than do rough-textured, angular particles. The test was performed by placing a 0.11-lb sample of a one-sized fraction of aggregate (passing No. 20 and retained on No. 30 sieves) into a glass jar with a cone-shaped lid and orifice. The jar was inverted, the stopper in the orifice removed, and a timer started. The rate of flow for the sample was then compared to the rate of flow for standard Ottawa sand of the same gradation.

Void Ratio by Western Technologies

The test was performed by placing a known volume of a single aggregate fraction into a graduated cylinder in a standard manner. The void ratio was calculated from the measured and absolute volumes of the aggregate. The test was repeated for three different-sized aggregate fractions and an average void ratio was computed. The test was specifically designed to use material separated into individual fractions from a sieve analysis and does not require a specific amount of material for performance of the test.

Florida Bearing Ratio

This test (Indiana State Highway Commission Test Method Inc. 201-72) was used to determine the bearing value of a fine aggregate. Fine aggregate was mixed with water and compacted into a bearing cup in lifts with a specified compressive load. The filled bearing cup was placed in a compression testing machine and given final compaction up to 1,500 lb at a rate of 2.4 in./min. The compacted specimen in the bearing cup was placed in the Florida bearing value machine with a 1-in.^{2} bearing plate centered on the specimen. A compressive load was applied to the bearing plate by a flow of steel shot at a standard rate. When the rate of deformation of the specimen reached 0.01 in. in 5 sec, the loading was discontinued and the weight of shot up to that moment was measured. The bearing ratio was calculated from the weight of shot.

Direct Shear Test

This test method was used to measure the internal friction angle of a fine aggregate under different normal stresses. A prepared sample of an aggregate was consolidated in a shear mold. The sample was then placed in a direct shear device and sheared by a horizontal force while applying a known normal stress. Other samples of the same aggregate were prepared and tested in the same manner under different normal stresses. The normal stresses and maximum shear stresses were plotted and the internal friction angle was measured.

Specific Rugosity by Packing Volume

A pouring test was used for direct measurement of the packing specific gravity of one-sized aggregate particles. Each of four different aggregate particle sizes was placed in a cone-shaped bin and then poured into a calibrated constant-volume container. The surface of the aggregate was leveled, the container and aggregate weighed, and the packing specific gravity computed. The macrosurface and microsurface voids were calculated using the apparent, bulk, and packing specific gravities. The specific rugosity was computed by adding the macrosurface and microsurface voids.

Asphalt Concrete Mix Design

Asphalt concrete mix designs were prepared for the various aggregate combinations by the Marshall method, using 75 blows per specimen face. The aggregate proportions are shown in Table 3; the aggregate gradations are shown in the following table.

Sieve Size	*Percent Passing*
3/4 in.	100
1/2 in.	92
3/8 in.	82
1/4 in.	70
No. 4	62
No. 8	47
No. 16	33
No. 20	23
No. 50	15
No. 200	5

Triplicate specimens were prepared for each aggregate combination studied by adding from 4 to 6 percent of the once-heated AC-20 asphalt cement. Coarse aggregate (CA) from each source was mixed with crushed fine aggregate (CFA) from the same source. When mixes utilized uncrushed fine aggregate (UFA), it was aggregate from the Tucson source regardless of the source of crushed aggregate. Specimens were compacted at 280°F with a mechanized compactor.

Specimens were extruded from their molds, cooled, and then weighed in air and in water. Specimens were then placed in a 140°F water bath for 30 to 40 min and tested for stability

TABLE 3 MARSHALL MIX DESIGN

	Crushed Fine Aggregate (%)	Aggregate Proportions (%)[a]		
		CA	CFA	UFA
Salt River Aggregate Pit	100	38.0	62.0	0
	67	38.5	41.6	19.9
	33	38.8	20.9	40.3
	0	39.8	0	60.2
Tucson Aggregate Pit	100	38.0	62.0	0
	67	38.1	41.3	20.6
	33	38.3	20.4	41.3
	0	38.7	0	61.3
Flagstaff Aggregate Pit	100	37.4	62.6	0
	67	38.4	43.1	18.5
	33	39.5	22.1	38.4
	0	41.4	0	58.6

[a]See text for aggregate gradations.

and flow in a Marshall test machine. Air voids, voids in mineral aggregate (VMA), voids filled with asphalt, and asphalt absorption were calculated using the mixture proportions, the bulk specific gravities of the specimens, and the maximum specific gravities of the mixtures.

Asphalt Concrete Strength and Deformation Tests

Tests of strength and deformation of compacted asphalt concrete were performed to develop data on the effect of crushed fine aggregate on these properties. Testing was performed on mixtures using the three aggregate sources and at two asphalt contents: (a) the asphalt content needed to produce 4 percent air voids, and (b) these asphalt contents plus 0.5 percent. This procedure was designed both to measure the effect of crushed fine aggregate on the strength and deformation of asphalt concrete and to obtain an indication of the effect of an increase of 0.5 percent in the asphalt content.

Tests performed to measure strength and deformation properties were the Hveem stability, resilient modulus, and two static creep tests. The two creep tests, one axial and one diametral, were both performed at 140°F. The axial creep test was also performed at 77°F. Only the Hveem stability test produced usable data. The diametral creep often exceeded the capacity of the deformation measuring device, resulting in incomplete data. The axial creep tests were not reproducible, which was believed to be the result of either deficient equipment or testing techniques. Time and funding did not permit further development of the creep testing. The small strains developed during resilient modulus testing are believed to be less than required to mobilize the effects of aggregate particle interaction; as a result, the resilient modulus is mostly a measure of the stiffness of the bituminous binder. It would not be expected to be significantly affected by aggregate shape and surface texture.

Triplicate specimens representing each of the aggregate sources, each of the crushed fine aggregate levels, and the two asphalt contents (at 4 percent air voids and 0.5 percentage points greater) were compacted with the kneading compactor (ASTM D-1561). Specimens were then tested for Hveem stability by ASTM Test Method D-1560.

TEST RESULTS

Aggregate Shape and Surface Texture

The seven test procedures for aggregate shape and surface texture for the three study sources were tested using fine aggregate with 100, 67, 33, or 0 percent crushed aggregate.

National Crushed Stone Association Procedure

This test procedure was performed using three replications of each test. The tests were performed using aggregate fractions from mechanical sieving. The sieve sizes used were No. 8 to No. 16, No. 16 to No. 30, and No. 30 to No. 50. The percent voids were calculated using the bulk specific gravity of the aggregate and the unit weights of the three aggregate fractions. The final test results are the averages of the results for the three aggregate fractions. An analysis of variance and the F-test indicated highly significant differences between the results of tests for individual aggregate sources and for percentage of crushed aggregate. Figure 1 is a plot of the mean result of each of the test variables for the National Crushed Stone Association procedure.

Index of Particle Shape and Texture

This test procedure used six different aggregate fractions, and each fraction was compacted by two different compactive efforts. The six sieve groups used were No. 4 to No. 8, No. 8 to No. 16, No. 16 to No. 30, No. 30 to No. 50, No. 50 to No. 100, and No. 100 to No. 200. Because of the amount of testing to obtain a single data point, replications of the test results were not performed, and data points are a single value. The test results are plotted in Figure 2. A definite relationship between particle index and amount of crushed aggregate existed. Results indicated the Tucson source to have considerably lower voids than the other two sources. The Salt River and Flagstaff particle indexes were only slightly different; however, the Flagstaff source had a lower particle index for all test results.

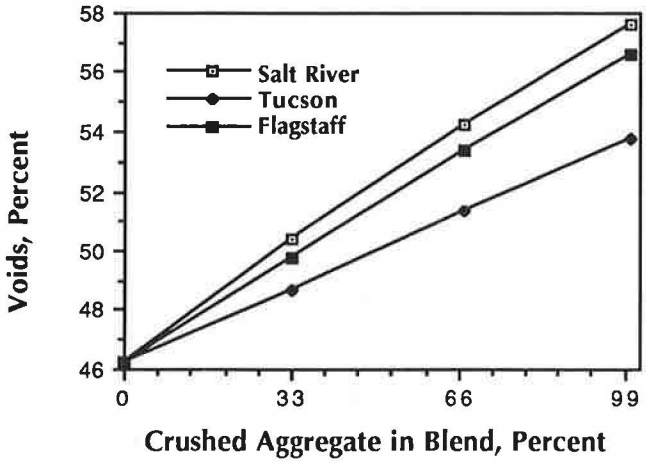

FIGURE 1 Results of National Crushed Stone Association procedure.

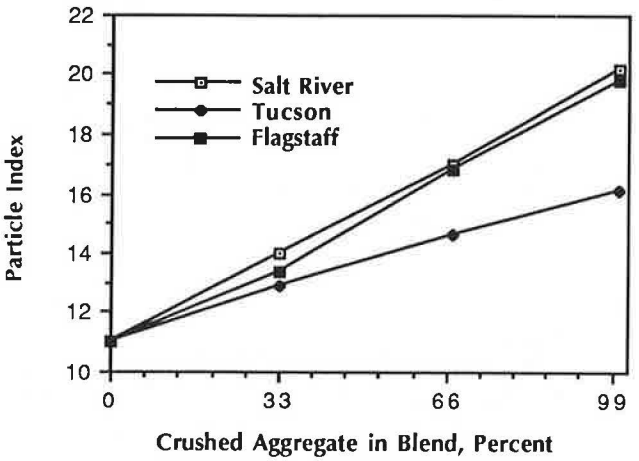

FIGURE 2 ASTM particle index.

Rex and Peck Time Index

The time index test used only a single aggregate fraction. This aggregate fraction was from between the No. 20 and No. 30 sieves. Three replications of the test were performed for each test variable. The average results of these tests are plotted in Figure 3. Statistical tests indicate highly significant differences for both aggregate sources and percentage of crushed aggregate. The order of time index for the three aggregate sources is the same as for the previous two test procedures but indicates the Flagstaff source to be about equidistant between the Salt River and Tucson sources, instead of nearer the Salt River source, as was shown by the other two tests.

Void Ratio by Western Technologies

Three replications were used for each test variable when this test was performed. Three sieve groups (No. 4 to No. 8, No. 20 to No. 30, and No. 100 to No. 200) were tested, and the three results were averaged for each replication. The results of the tests appear in Figure 4. Significant differences between aggregate sources and amounts of crushed aggregate resulted, and the order of void ratios for the three sources was found to be the same order as test results from the prior three tests.

Florida Bearing Value

Three replications of all test variables were performed for the Florida bearing value test. However, test results for both the Salt River and Flagstaff sources exceeded the capacity of the apparatus when using more than 33 percent crushed aggregate. The Tucson source had Florida bearing ratios below the other two sources and was the only source that remained within the capacity of the apparatus up to 100 percent crushed aggregate. The results of tests at 33 percent crushed aggregate indicated a higher value for the Flagstaff source than the Salt River source. This is different from the four tests previously examined. The averages of the test results obtained appear in Figure 5.

Direct Shear Test

Three replications of the direct shear test were performed for each test variable. The test results showed no distinct rela-

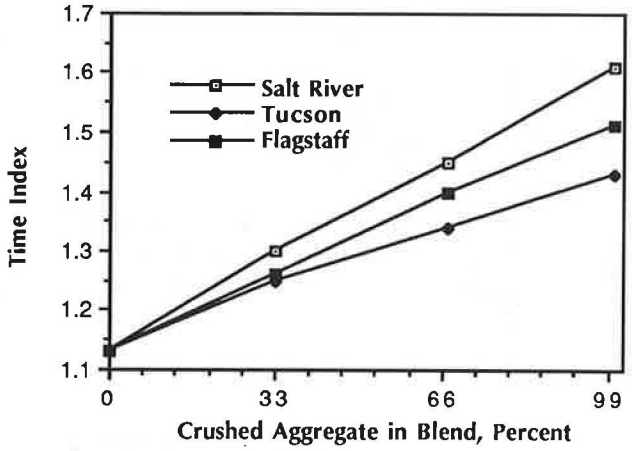

FIGURE 3 Rex and Peck time index.

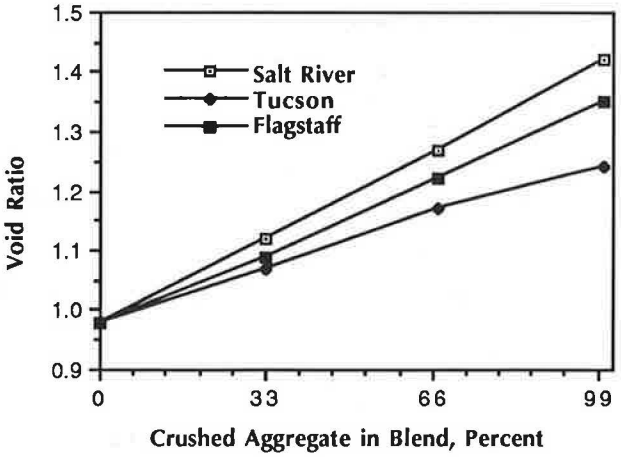

FIGURE 4 Western Technologies void ratio.

tionship for either the aggregate sources or the amount of crushed fine aggregate. The differences between friction angles measured were quite small, with all test results falling between 42 and 45 degrees. The results of the direct shear test appear in Figure 6.

Specific Rugosity by Packing Volume

Three replications of the packing volume were performed. The test procedure used four aggregate fractions: No. 8 to No. 10, No. 20 to No. 30, No. 60 to No. 80, and No. 200 to No. 270. The results of the packing specific gravity for the test variables studied are shown in Figure 7. Unique relationships exist for each of the aggregate sources, and the packing specific gravities are related to the amount of crushed aggregate. The arrangement of the relationships is quite different from the other tests performed. This is a result of the differences in specific gravity of aggregate from the three sources.

The macrosurface voids and microsurface voids were calculated using the apparent, bulk, and packing specific gravities for each aggregate combination. The averages of the

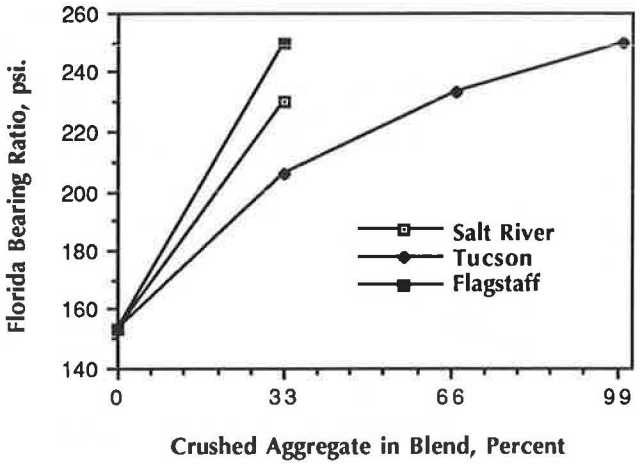

FIGURE 5 Florida bearing ratio.

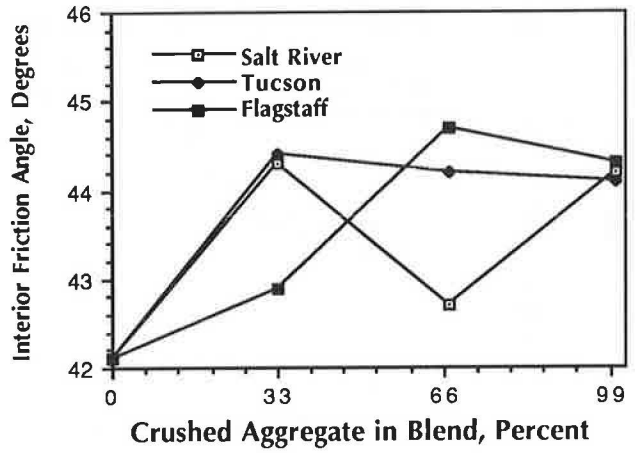

FIGURE 6 Direct shear.

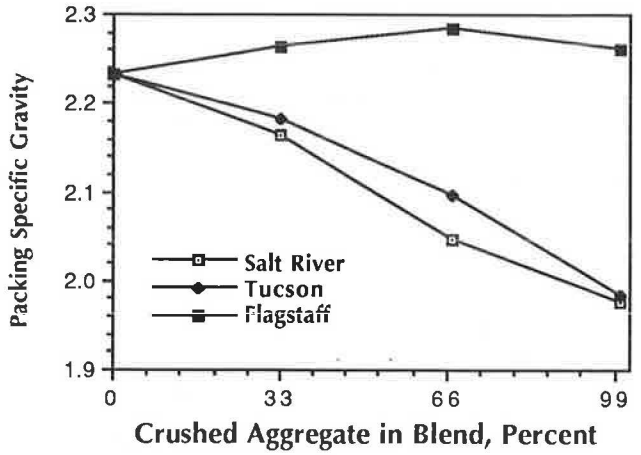

FIGURE 7 Packing specific gravity.

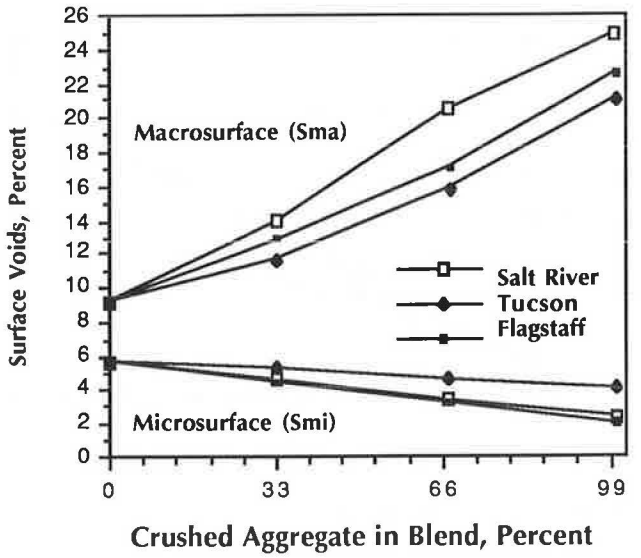

FIGURE 8 Microsurface and macrosurface voids.

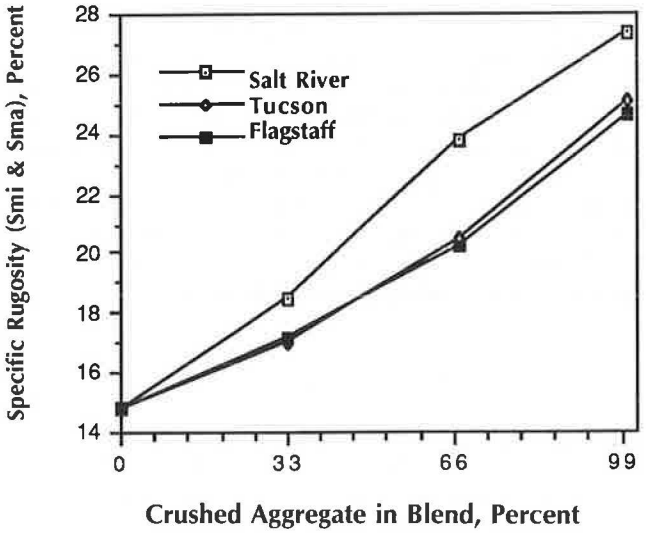

FIGURE 9 Specific rugosity.

results of these calculations are shown in Figure 8. Although relationships between the voids and the percentage of crushed aggregate appear to exist, the order for the aggregate sources shows no relation to that demonstrated by other tests.

The specific rugosity is the sum of the macrosurface and the microsurface voids. The specific rugosities for the study variables appear in Figure 9. Statistical tests indicated significant differences for percentage of crushed aggregate and also significant differences for aggregate sources. It is apparent from Figure 9 that the significant difference for aggregate sources was the result of the Salt River source being different from the Tucson and Flagstaff sources, which had almost identical test results.

Asphalt Concrete Mix Design

Mix designs were performed using the Marshall method with 75 compactive blows per specimen face. Asphalt cement was AC-20. Four mix designs were prepared for each of the three sources of aggregate, using that source's coarse aggregate and four different combinations of crushed and uncrushed aggregate. Crushed fine aggregate was from the same source as the coarse aggregate, and uncrushed fine aggregate was from the Tucson source. Aggregate combinations were adjusted for bulk specific gravity to provide a constant gradation by volume. A summary of the aggregate combinations, the percent by weight for each of the aggregates, and the combined gradation was previously shown in Table 3.

Mixtures were prepared and compacted at four or more asphalt contents for each aggregate source. The asphalt content that would yield approximately 4 percent air voids was selected for use in further testing. These asphalt contents are referred to as the optimum asphalt content for the remainder of this paper. The asphalt contents selected and the physical properties of the mixtures at those values are shown in Tables 4, 5, and 6.

Asphalt Concrete Strength and Deformation Tests

A series of tests was performed using asphalt concrete specimens with the various aggregate combinations at both the optimum asphalt content and at an asphalt content 0.5 percentage points greater. Specimens for static creep testing at 77°F and 140°F were compacted by the Marshall method with 75 compactive blows per specimen face. Another series of specimens was compacted with the kneading compactor. These specimens were initially tested for Hveem stability. Later they were tested for resilient modulus at 77°F, following which they were tested for diametral creep at 140°F. Only the Hveem stability test results are presented and discussed.

Data from the Hveem stability tests are shown in Table 7. Statistical tests indicate highly significant differences in test results for different percentages of crushed fine aggregate and different sources, with a significant difference between tests at the two different asphalt contents. Stabilities generally decreased with decreases in the percentage of crushed fine aggregate and with the 0.5-percentage-point increase in asphalt content. The Flagstaff source demonstrated higher Hveem stabilities than the other two sources, which were not significantly different from each other.

TABLE 4 ASPHALT MIX DESIGN PROPERTIES (SALT RIVER AGGREGATE)

	Salt River Aggregate			
	Nominal Percent Crushed Fine Aggregate			
Test Property	100	67	33	0
Asphalt Content, BTW, %	6.1	5.3	5.1	5.4
Bulk Unit Wt, pcf	146.4	146.6	145.9	144.5
Max Unit Wt, pcf	152.5	152.7	152.0	151.4
VMA, %	17.0	14.0	14.2	15.0
Voids Filled, %	76	71	72	68
Air Voids, %	4.0	4.0	4.0	4.6
Stability, lb	3340	3380	3770	3250
Flow, 0.01 in.	14	10	11	12

TABLE 5 ASPHALT MIX DESIGN PROPERTIES (TUCSON AGGREGATE)

	Tucson Aggregate			
	Nominal Percent Crushed Fine Aggregate			
Test Property	100	67	33	0
Asphalt Content, BTW, %	6.2	5.8	5.7	5.4
Bulk Unit Wt, pcf	141.7	142.5	143.0	143.7
Max Unit Wt, pcf	147.6	148.5	149.0	149.8
VMA, %	15.3	14.6	14.2	14.6
Voids Filled, %	74	73	61	66
Air Voids, %	4.0	4.0	4.0	4.7
Stability, lb	3620	3450	3720	3920
Flow, 0.01 in.	14	11	10	10

TABLE 6 ASPHALT MIX DESIGN PROPERTIES (FLAGSTAFF AGGREGATE)

	Flagstaff Aggregate			
	Nominal Percent Crushed Fine Aggregate			
Test Property	100	67	33	0
Asphalt Content, BTW, %	5.7	5.5	5.4	5.3
Bulk Unit Wt, pcf	159.8	157.2	152.4	149.2
Max Unit Wt, pcf	167.5	162.9	158.1	155.5
VMA, %	16.5	15.5	15.0	14.0
Voids Filled, %	76	73	74	71
Air Voids, %	4.1	4.1	3.7	4.0
Stability, lb	3800	3400	3700	3380
Flow, 0.01 in.	12	11	10	10

TABLE 7 HVEEM STABILITY

		Percent Crushed							
		100		67		33		0	
Aggregate Pit	Trial	I	II	I	II	I	II	I	II
Salt River	1	31	18	30	24	31	31	28	21
	2	35	23	31		20	34	29	20
	3	27	26	35	35	31	24	21	25
	Mean	31	22	32	30	27	30	26	22
Tucson	1	31	36	29	33	19	24	22	19
	2	47	29	31	31	22	22	24	30
	3	42	33	29	27	28	23	22	25
	Mean	40	33	30	30	23	23	23	25
Flagstaff	1	42	32	37	44	32	30	34	31
	2	38	34	34	32	24	21	26	23
	3	44	33	32	25	27	31	32	21
	Mean	41	33	34	34	28	27	31	25

Notes: (1) I - Optimum asphalt content at 4% air voids
(2) II - Optimum asphalt content plus 0.5%
(3) Data are Hveem stabilities

Aggregate-Asphalt Concrete Relations

Three of the aggregate shape and texture tests (National Crushed Stone Association procedure, Rex and Peck time index, and specific rugosity) were selected to examine a relationship to Hveem stability. The best-fit straight lines were computed using a least-squares linear regression analysis. The results of these analyses are shown in Figures 10, 11, and 12. The relationships developed have values for R (coefficient of correlation) from 0.78 to 0.89. These correspond to coefficients of determination from 0.61 to 0.79. These values indicate that the relationships are a good fit for the data and that there is a good correlation between the variables being tested.

DISCUSSION OF TEST RESULTS

Aggregate Shape and Surface Texture

The results of the aggregate shape and surface texture testing were examined to select the most practical tests for routine use that also gave reliable data. Of the seven test procedures studied, only the direct shear test failed to differentiate between either percentage of crushed fine aggregate or aggregate source. The Florida bearing value had incomplete data due to the inability to reach failure loads for some tests. The ASTM particle index was found to be very labor-intensive and time-consuming; it is more practical for special studies than for routine testing. The Western Technologies Inc. void test has not been researched sufficiently to be accepted at this time.

The three remaining test procedures (National Crushed Stone Association procedure, Rex and Peck time index, and specific rugosity) were found to be the preferred tests. Specific rugosity involves the development of both microsurface and macrosurface voids that should be examined; however, the specific rugosity was considered to be the most valuable test result. The Rex and Peck time index has the disadvantage that it uses only a single aggregate fraction and may not always be representative of the character of the entire fine aggregate. These three tests were selected to correlate with the results of asphalt concrete strength and deformation test results.

Asphalt Concrete Mixtures

The results of mix design testing were summarized in Tables 4, 5, and 6. The properties shown are the results of the mix design at approximately 4 percent air voids. Some trends in

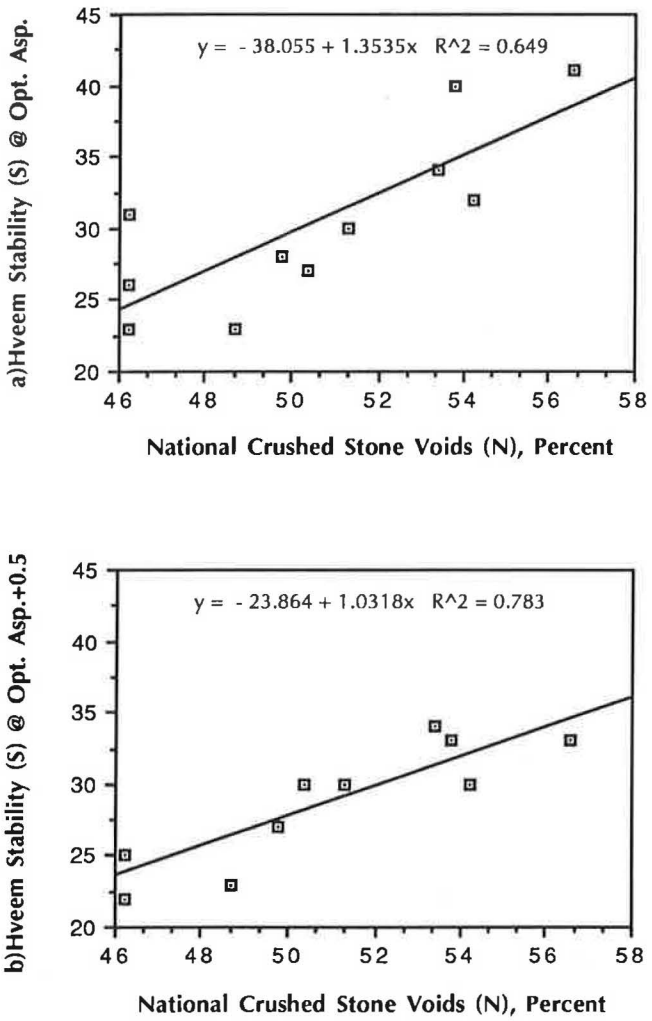

FIGURE 10 Hveem stability–National Crushed Stone Association procedure relationships.

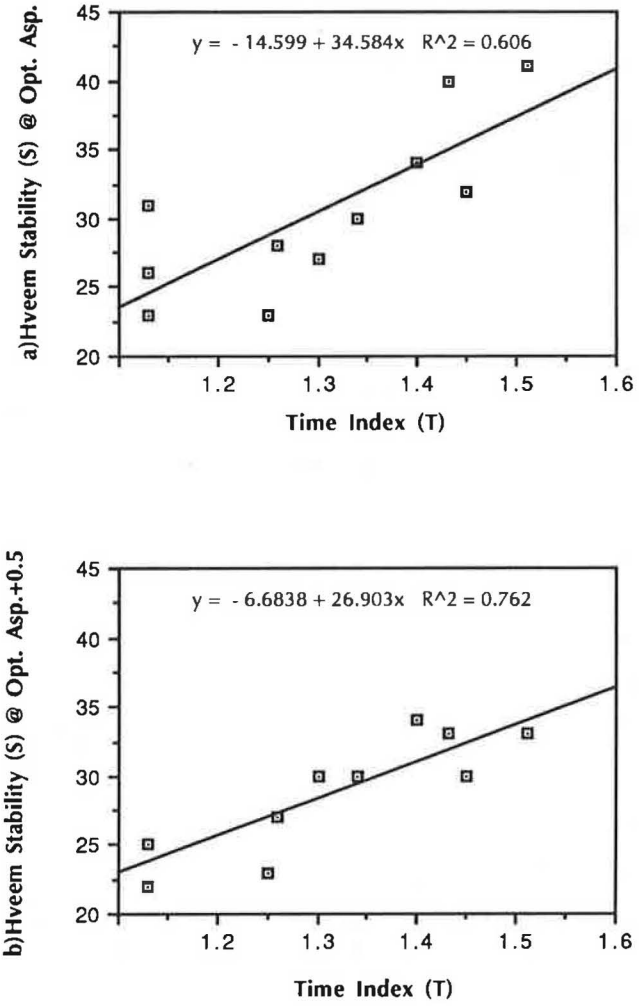

FIGURE 11 Hveem stability–time index relationships.

the data related to percentage of crushed fine aggregate can be seen. The asphalt content and VMA generally increased with increasing amount of crushing. No trend in the Marshall stability could be noted; however, the flow tended to increase with increasing percentage of crushed fine aggregate. It would be expected that increased proportions of crushed fine aggregate would reduce flow, but the opposite occurred. Boutilier (*8*) concluded that particle index had no effect on flow. Trends shown in bulk and maximum unit weights are the result of the variation in specific gravity between the crushed fine aggregate and the uncrushed Tucson aggregate, instead of the amount of fine aggregate crushing.

Asphalt Concrete Strength and Deformation Tests

Only the Hveem stability was found to have a good relationship to the percentage of crushed fine aggregate. It is felt that creep test results would be influenced by the percentage of crushed fine aggregate; however, problems resulting in performance of the creep testing prevented the acquisition of good data for this study. The resilient modulus data did not correlate with the percentage of crushed fine aggregate. It is believed that resilient modulus is more closely related to the properties of the binder than the aggregate.

The static creep tests at 77°F and 140°F did not provide reproducible test results, and the data showed no relationship to the variables being studied. Likewise, the diametral creep tests at 140°F did not prove useful, partially because of a lack of reproducibility and partially because the permanent deformation often exceeded the range for the measuring equipment. It is believed that creep testing should show a good correlation to the degree of crushing in the fine aggregate of an asphalt concrete and that the inability to obtain good creep data here should not lead to the conclusion that these variables are not related.

Aggregate-Asphalt Concrete Relationships

The relationships between Hveem stability and each of the three fine aggregate shape and surface texture tests selected for correlation were found to be good. Any one of these tests (National Crushed Stone Association, Rex and Peck time

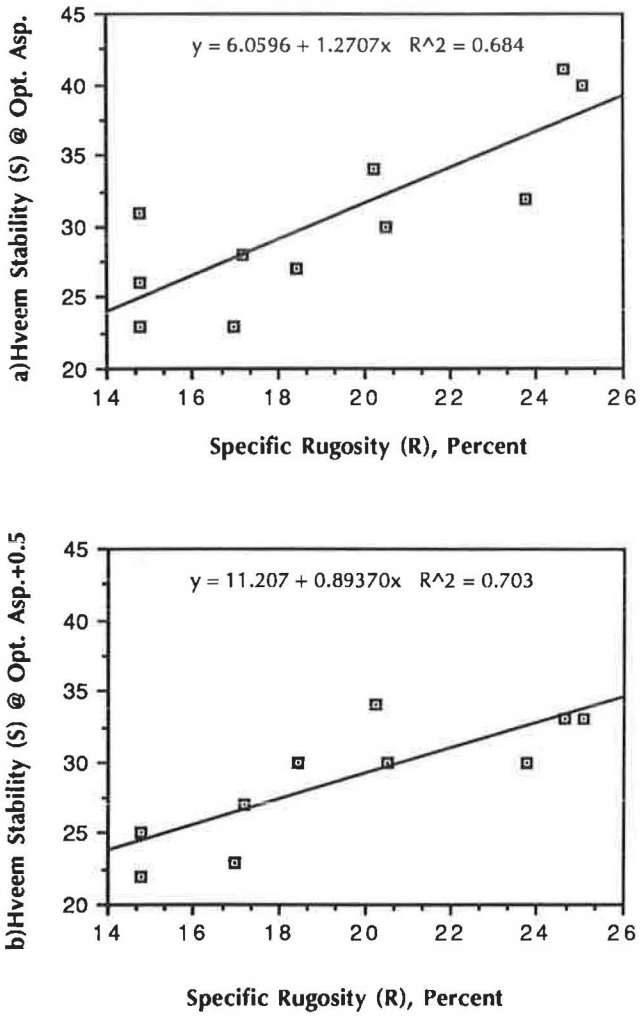

FIGURE 12 Hveem stability–specific rugosity relationships.

index, or specific rugosity) could be used to screen fine aggregate properties for use in asphalt concrete mixtures.

CONCLUSIONS

The shape and surface texture of fine aggregate can be evaluated by a number of tests. Seven tests were studied and results of all but direct shear were found to be related to the proportion of the fine aggregate with crushed faces.

Asphalt concrete mixture properties were affected by the percentage of fine aggregate with fractured faces resulting from aggregate crushing. Voids in mineral aggregate increased with increasing percentage of crushed fine aggregate, which resulted in increased asphalt content to achieve 4 percent air voids.

The Hveem stability of asphalt concrete mixtures was found to be linearly related to the results of tests of fine aggregate shape and surface texture.

ACKNOWLEDGMENTS

The authors recognize the Arizona Department of Transportation and Federal Highway Administration for their support for this study. Particular recognition should go to Frank McCullagh of the Arizona Transportation Research Center and his staff for their assistance and support.

REFERENCES

1. M. Herrin and W. H. Goetz. Effect of Aggregate Shape on Stability of Bituminous Mixes. *HRB Proc.*, Vol. 33, 1954, pp. 293–308.
2. H. M. Rex and R. A. Peck. A Laboratory Test to Evaluate the Shape and Surface Texture of Fine Aggregate Particles. *Public Roads*, Dec. 1956.
3. E. Y. Huang. An Improved Particle Index Test for the Evaluation of Geometric Characteristics of Aggregates. *ASTM Journal of Materials*, Vol. 2, No. 1, March 1987.
4. E. Tons and W. H. Goetz. Packing Volume Concept for Aggregates. *Highway Research Record 236*. HRB, National Research Council, Washington, D.C., 1968, pp. 76–92.
5. I. Ishai and E. Tons. A Concept and a Test Method for a Unified Characterization of the Geometric Irregularity of Aggregate Particles. *ASTM Journal of Testing and Evaluation*, Vol. 5, No. 1, Jan. 1977.
6. N. W. McLeod and J. K. Davidson. Particle Index Evaluation of Aggregates for Asphalt Paving Mixtures. *Proc.*, AAPT, Vol. 50, 1981.
7. J. M. Griffith and B. F. Kallas. Influence of Fine Aggregate on Asphaltic Concrete Paving Mixtures. *HRB Proc.*, Vol. 37, 1958, pp. 219–255.
8. O. D. Boutilier. A Study of the Relation Between the Particle Index of the Aggregate and the Properties of Bituminous Aggregate Mixtures. *Proc.*, AAPT, Vol. 33, 1967, pp. 157–179.
9. I. Ishai and E. Tons. Aggregate Factors in Bituminous Mixture Design. Report 335140-1-F. University of Michigan, Ann Arbor, Mich., 1971.
10. I. V. Kalcheff and D. G. Tunnicliff. Effects of Crushed Stone Aggregate Size and Shape on Properties of Asphalt Concrete. *Proc.*, AAPT, Vol. 51, 1982.
11. I. Ishai and H. Gelber. Effect of Geometric Irregularity of Aggregates on the Properties and Behavior of Bituminous Concrete. *Proc.*, AAPT, Vol. 51, 1982.

$Ca(OH)_2$ Treatment of Crushed Limestone Base Course Materials for Determination of Self-Cementation Potential

ROBIN E. GRAVES, JAMES L. EADES, AND LARRY L. SMITH

Highway base course materials composed of crushed limestone aggregates have been observed to increase in strength with time under both field and laboratory conditions. Studies have shown that this is due primarily to the movement of Ca^{2+} and CO_3^{2-} ions, which produces a natural cementation process in these materials. Testing of materials with variable silica-carbonate compositions indicated that the amount of strength developed from the carbonate cementation process is a function of the mineralogic composition of the materials, with more strength developed as calcium carbonate composition increased. Scanning electron microscopic studies suggest that this is due to differences in bonding characteristics between calcite cement–calcite particle and calcite cement–quartz particle systems. Treatment of the silica-carbonate materials with $Ca(OH)_2$ (hydrated lime) before testing enhanced strength development by furnishing Ca^{2+} ions, which carbonate to form an additional source of calcium carbonate cement. This treatment allows for a more rapid test method to determine the potential strength development in silica-carbonate materials from natural cementation processes.

The Florida Department of Transportation has investigated the strength increase observed in highways constructed with crushed limestone base course materials through both laboratory studies (*1–3*) and satellite road projects. The research has indicated that the strength development occurs because of a slight drying of the base course (*2*) and dissolution and reprecipitation of fine carbonate particles, which serve as a cementing agent within the base course (*1,3*).

Calcium carbonate is a very common cementing agent in natural geological materials due to its high susceptibility to dissolution and precipitation under the range of physical and chemical conditions encountered on and within the earth (*4*). Since highways are constructed at the earth's surface, they are subjected to fluctuating environmental conditions such as temperature and atmospheric pressure. Therefore, the engineering behavior of base courses composed of calcium carbonate materials may be influenced by cementation processes operating within them.

Cementation of the particles provides a cohesive component to the system (*5,6*), thereby increasing the overall strength of the soil mass. Therefore, natural cementation of particles within a highway base course could cause an increase in strength of the material with time as cementation progresses.

High-carbonate-composition base course materials have traditionally been preferred for construction of state highways in Florida. However, as sources of these materials are depleted, new sources must be found to accommodate the transportation needs of the state's rapidly expanding population. This often results in a change in mineralogical properties and performance. Materials currently obtained from the newer quarries sometimes contain abundant unconsolidated quartz sand, and several instances of deterioration have occurred in county-built roads that used the high-silica materials for the base course.

Research was conducted to determine the effects of high silica composition in these materials on the carbonate cementation process and the resulting strength development (*3*). From this research, a test method has been devised involving $Ca(OH)_2$ treatment of silica-carbonate materials that enables a more rapid evaluation of potential strength development from natural cementation processes.

STRENGTH TESTING METHODS AND MATERIALS

The testing program utilized Limerock Bearing Ratio (LBR) tests (*7*) on materials of varying quartz-calcite composition in order to determine strength changes as a function of sample composition and time. The standard LBR test method involves compacting materials into 6-in. molds at modified AASHTO compactive efforts and then soaking the compacted materials in water for 48 hr. The materials are then removed from the water and penetrated by a loading device, with an LBR value calculated as follows:

$$\text{LBR} = \frac{\text{Unit load (psi) at 0.1-in. penetration}}{800 \text{ psi}} \times 100 \qquad (1)$$

The test is performed at different water contents, and the maximum LBR value is taken. The LBR test is similar to the more commonly used California Bearing Ratio (CBR) test. An approximate correlation has been established between the two methods, with an LBR value of 100 corresponding to a CBR value of 80.

R. E. Graves and J. L. Eades, Department of Geology, University of Florida, Gainesville, Fla. 32611. L. L. Smith, Florida Department of Transportation, 2006 N.E. Waldo Rd., Gainesville, Fla. 32602.

Sand Mixes

Quartz and calcite sands were mixed in various proportions, resulting in compositional quartz-to-calcite ratios of 0:100, 25:75, 40:60, 50:50, 60:40, 75:25, and 100:0. The various mixes were compacted into LBR molds at maximum Modified Proctor densities and continuously soaked in water at room temperature (70° ± 2°F) for time intervals of 2, 7, 14, 30, and 60 days before testing. Continuous soaking of the samples was performed, because a previous study (*1*) showed that this method is more efficient for producing carbonate cementation in the laboratory than using wetting and drying cycles.

Figure 1 shows the LBR values for 7-, 14-, 30-, and 60-day soaking periods, relative to the standard 2-day soak, for the various sand mix compositions. LBR values for the extended soaking periods are plotted as percentage increases over the 2-day reference LBR for each compositional mix. The graph illustrates the differences in strength development as composition varied. Low-carbonate sands (0 and 25 percent calcite) show no strength increase up to 60 days soaking, while higher carbonate sands (40 to 100 percent calcite) showed strength increases, with more strength developed as carbonate content increased.

Maximum increase was obtained after 14 days soaking, with no additional strength developed for 30- and 60-day soaking periods. This may be related to the small amount (less than 2 percent) of fine-grained material (passing Number 200 sieve) in the carbonate sand. Dissolution of small carbonate particles is likely to be more efficient than coarser particles due to higher surface area available in fine-grained materials. It is possible that the fine carbonate particles have been "used up" in the cementation process after 14 days and that the coarser particles are not providing cementing material as efficiently. It is suspected that coarser carbonate particles would provide cementing material over longer periods of time, but at a slower rate due to less available surface area for dissolution and the smaller amount of water held by large particle contacts.

Cemented Coquina

Cemented coquina base course materials mined from the Anastasia Formation on the east coast of Florida were also compacted, continuously soaked, and tested to compare with sand mix data. Compositional variation was more limited in these materials, with quartz-to-calcite ratios of 45:55, 55:45, and 65:35 used for testing. Soaking periods of 2, 7, 14, and 30 days were used, with the 60-day soaking periods omitted because of a limited amount of sample material.

LBR data for soaked and tested cemented coquina materials also indicate differential strength development as composition varied. Figure 2 shows percentage increase in strength of each composition for soaking periods of 7, 14, and 30 days relative to the standard 2-day soak LBR value. More strength was developed in the cemented coquina materials as carbonate content increased, as was the case for the quartz-calcite sand mixes. However, differences in the pattern of strength development can be seen when comparing the two materials. Cemented coquina materials continued to increase in strength up to 30 days soaking, while quartz:calcite sand mixes did not increase after soaking 14 days. This is thought to be due to slightly more carbonate fines (passing Number 200 sieve) occurring in the cemented coquina materials than in the sand mixes.

$Ca(OH)_2$ Treatment

Another objective of the research was to develop a test method for prediction of potential strength development in silica-carbonate materials. Previous work (*1*) using NaCl and CO_2 treatments showed that these methods did not significantly increase cementation in the laboratory over that derived from soaking in plain water. Therefore, another treatment method was investigated by mixing 1 percent $Ca(OH)_2$ (hydrated lime) to the dry materials before compacting and soaking. This was done in an attempt to enhance carbonate cementation and, therefore, strength development. Carbonation of additional Ca^{2+} ions furnished by the $Ca(OH)_2$ should provide an additional source of calcite cement, thereby enhancing cementation effects.

Figure 3 shows the LBR values for 2-, 7-, 14-, 30-, and 60-day soaking periods on the quartz-calcite sand mixes treated with 1 percent $Ca(OH)_2$ before compacting, compared to the standard 2-day soak on untreated sand mixes. The graph illustrates the effects of an additional source of carbonate cement on strength increase with time and compositional variation of the mixes. It indicates that $Ca(OH)_2$ treatment significantly

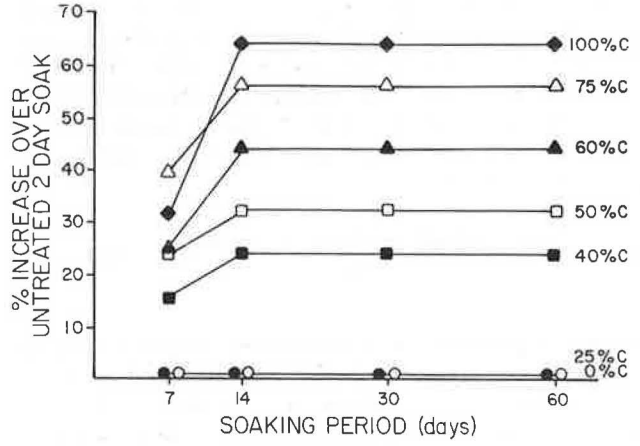

FIGURE 1 Strength increase of untreated quartz-calcite sand mixes.

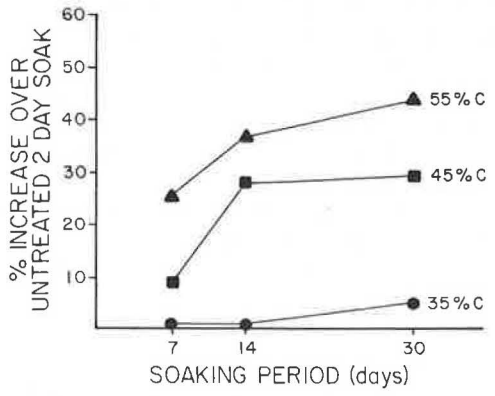

FIGURE 2 Strength increase of untreated cemented coquina materials.

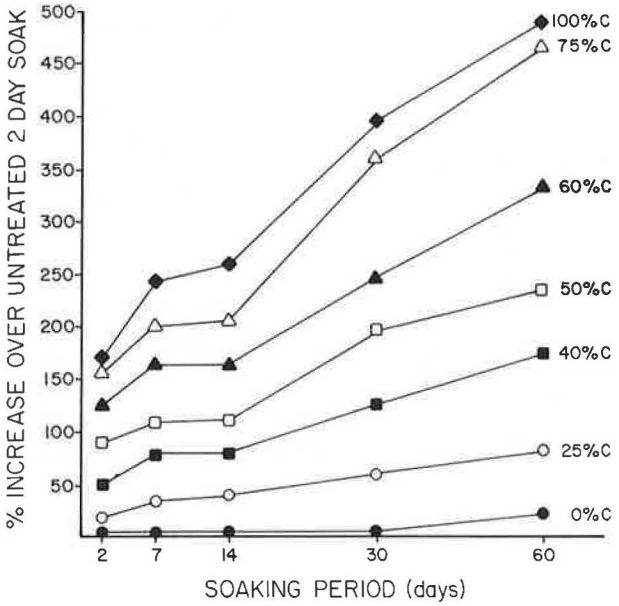

FIGURE 3 Strength increase of quartz-calcite sand mixes treated with 1 percent $Ca(OH)_2$.

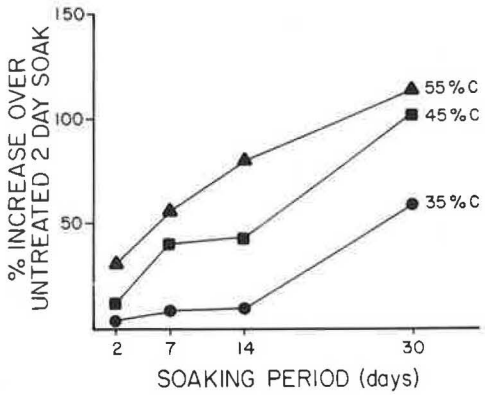

FIGURE 4 Strength increase of cemented coquina materials treated with 1 percent $Ca(OH)_2$.

enhanced strength development and variational patterns observed in LBR data for the untreated sand mixes. Very large increases (more than 450 percent) in strength occurred for high-carbonate sands, with strength developed continuously up to 60 days. Less strength was developed in the sand mixes as carbonate content decreased. Quartz sands developed no additional strength after 30 days soaking and only a slight increase (30 percent) after 60 days soaking.

Treatment of the cemented coquina materials with 1 percent $Ca(OH)_2$ also resulted in enhanced cementation effects. Figure 4 shows strength increase for each composition after soaking periods of 2, 7, 14, and 30 days, relative to the standard untreated 2-day soak LBR values. More strength was developed when cemented coquina materials were treated with $Ca(OH)_2$, with the trend of more strength developed with increasing carbonate composition persisting in these experiments.

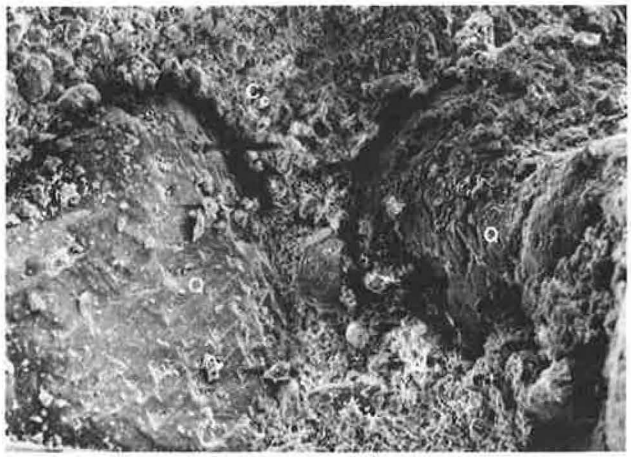

FIGURE 5 Sand mix, 75 percent carbonates, 1 percent $Ca(OH)_2$, 14-day soak (303×).

SEM EXAMINATIONS

Scanning electron microscope (SEM) examinations were conducted on tested LBR materials to aid in explanation of strength testing data by observing cementation characteristics. Samples of the LBR materials were removed from the molds after soaking and testing, dried, and prepared for SEM analysis.

The micrographs presented in Figures 5 and 6 show the different characteristics between carbonate cementation of quartz and calcite particles in the quartz-calcite sand mixes. In Figure 5, the carbonate cement (C_c) has not bonded to the quartz particles (Q), as evidenced by the clean quartz particle surfaces and the large void separating the particles and cement. In contrast, Figure 6 shows a calcite particle (C_p) which seems to be well bonded to the carbonate cement (C_c). Carbonate cementing material has adhered to the particle surface during fracture, and the cement is in good contact around the calcite particle edges.

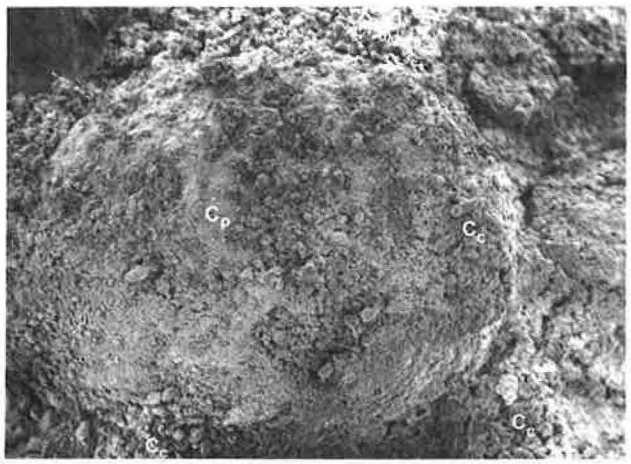

FIGURE 6 Sand mix, 100 percent carbonates, 1 percent $Ca(OH)_2$, 14-day soak (141×).

Higher magnification micrographs of cement-particle contacts for quartz and calcite particles are shown in Figures 7 and 8. The carbonate cement (C) and quartz particle (Q) are separated by a void in Figure 7. Note the arrows where small carbonate particles have been cemented together. Figure 8 shows carbonate cement (C_c) bonded to a large carbonate particle (C_p).

Similar cementation characteristics were observed in examination of cemented coquina LBR materials after soaking and testing. In Figure 9, calcite particles (C) are well cemented, while quartz particles (Q) exhibit clean particle surfaces, free of carbonate cement.

Naturally occurring calcite-cemented quartz sandstones from the Badlands of South Dakota were also examined to observe cement-particle contacts of materials in more advanced stages of cementation. Figure 10 is a micrograph of a fractured surface of the material showing the quartz particles (Q) in a calcite cement matrix (C). The cement has pulled away, leaving clean quartz particle surfaces, and large voids exist at the cement-particle interface.

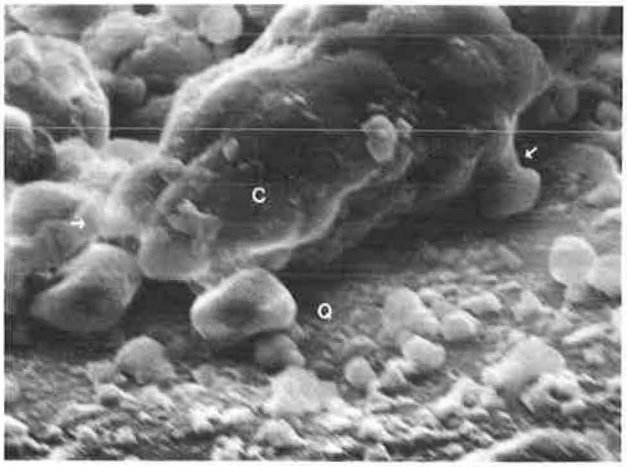

FIGURE 7 Sand mix, 25 percent carbonates, 7-day soak (1776×).

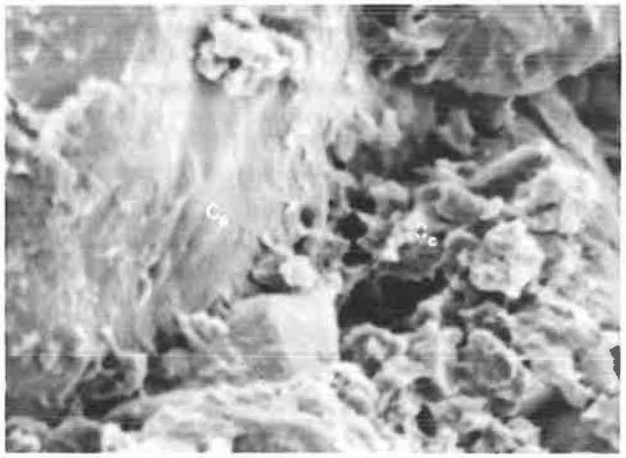

FIGURE 8 Sand mix, 100 percent carbonates, 1 percent $Ca(OH)_2$, 30-day soak (3552×).

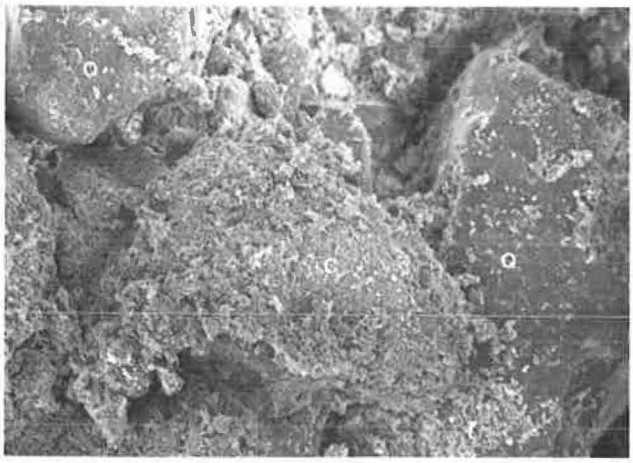

FIGURE 9 Cemented coquina, 45 percent carbonates, 1 percent $Ca(OH)_2$, 30-day soak (111×).

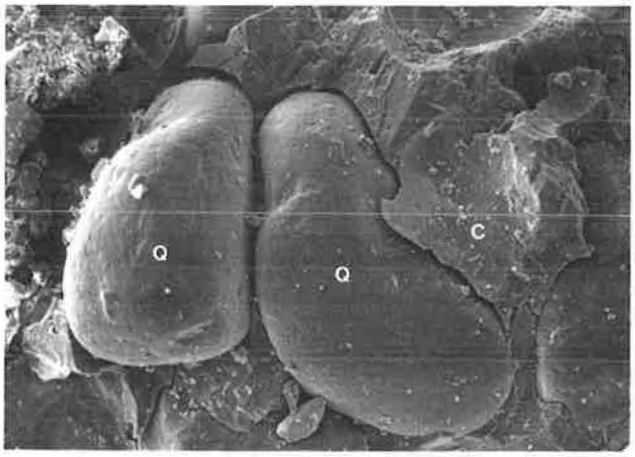

FIGURE 10 Calcite cemented quartz sandstone, Badlands, South Dakota (111×).

DISCUSSION OF RESULTS

The high susceptibility of calcium carbonate to dissolution and reprecipitation under normal physical and chemical conditions operating at the earth's surface was illustrated in the LBR testing program by the strength increases occurring in the laboratory samples after extended soaking in water. Because the samples remained at constant temperature (70° ± 2°F) during soaking, the cementation process operating within the samples is thought to be controlled by variations in atmospheric pressure. This would cause changes in the CO_2 content of the pore waters, which is the main controlling factor over carbonate dissolution and precipitation (*8,9*).

Differential strength gains as a function of mineralogical composition in the tested LBR materials, along with microscopic observations of the different bonding characteristics of carbonate cement to calcite and quartz particles, support the ideas on "compatible" and "incompatible" cements as put forth by Dapples (*10*) and others (*3,11,12*). Carbonate cementation of carbonate particles (compatible system) exhibited

much better cement-particle bonding than carbonate cementation of quartz particles (incompatible system). This was evidenced in the LBR testing program by the larger strength increases for high-carbonate samples as compared to high-silica samples.

Microscopic examinations supported LBR testing data by illustrating the different cement bonding characteristics as a function of cement-particle composition. Carbonate cement appears to nucleate directly onto calcite particle surfaces, creating a strong cement-particle bond. In the carbonate cement–quartz particle system, the cement seems to precipitate from solution into pore spaces without nucleation or bonding to the quartz particle surfaces. Examination of fractured surfaces of these materials illustrated this, with quartz particles exhibiting clean particle surfaces free of adhering cement, and voids existing between cement and particles at cement-particle contacts. This was in contrast to carbonate cementation of calcite particles. These particles appear to be well bonded to the cement, as evidenced by cement-covered particle surfaces and absence of voids at cement-particle contacts.

Treatment of both quartz-calcite sand mixes and cemented coquina materials with 1 percent $Ca(OH)_2$ before compacting and soaking the samples proved to be very effective in providing an additional source of carbonate cementing material, resulting in larger and more rapid strength increases than in untreated materials. These experiments also enhanced the effect of cement-particle composition, with more strength developed as carbonate composition of the samples increased. As discussed previously, the $Ca(OH)_2$ provides an additional source of Ca^{2+} ions, which form carbonate cementing material through carbonation of the Ca^{2+} ions during soaking. Calcium hydroxide has a solution pH of 12.4 at 25°C (*13*), which would increase CO_3^{2-} species of dissolved carbonate in the pore waters of the samples (*14*). The Ca^{2+} ions and CO_3^{2-} ions combine and precipitate as calcium carbonate cement, thus increasing the strength of the soaked materials.

The large strength increases obtained from $Ca(OH)_2$ treatment of high-carbonate samples suggests that this procedure may be useful for strength improvement of high-carbonate foundation materials and as an accelerated testing method for determination of potential self-cementation of silica-carbonate foundation materials. A suggested method of test would be as follows:

1. Mix 1 percent $Ca(OH)_2$ to dry materials before compaction into LBR (or CBR) molds at optimum water content.
2. Soak the compacted sample in water for 2 to 7 days.
3. Test the sample and compare to the standard 2-day soak LBR (or CBR) value for the untreated materials to determine a percentage increase in strength.

The strength developed in the treated sample should be indicative of the strength that would be developed in untreated materials soaked for 30 to 60 days. This treatment would greatly reduce the required soaking time, allowing for a more rapid test method for determination of potential strength development.

One problem with the test is that the soaking interval required for treated samples may vary among different types of materials because of differences in particle size and distribution. This may affect the amount of strength developed as a result of differences in compacted density and the amount of carbonate fines between various materials. Therefore, initial trial tests comparing treated and untreated materials may be required on a case-by-case basis for different types of materials in order to develop empirical relationships. Once a strength relationship has been developed for a particular type of material, the $Ca(OH)_2$ treatment method could be used routinely, thus avoiding the extensive soaking periods required to determine strength development in untreated silica-carbonate materials.

CONCLUSIONS

1. Continuous laboratory soaking of compacted quartz-calcite sand mixes and cemented coquina base course materials in plain water resulted in strength increases with time, except for samples of very high silica composition.
2. Higher strengths were developed in proportion to increasing calcium carbonate composition for both quartz-calcite sand mixes and cemented coquina base course materials.
3. Treatment of quartz-calcite sand mixes and cemented coquina base course materials with the addition of 1 percent $Ca(OH)_2$ before compacting and soaking proved to be an effective method of enhancing cementation effects on strength development by furnishing a more soluble source of Ca^{2+} ions, which form calcium carbonate cement through carbonation of the Ca^{2+} ions.
4. Treatment of high-carbonate materials with 1 percent $Ca(OH)_2$ greatly increased the rate and amount of their strength development, while treatment of high-silica materials resulted in little or no strength increase. This suggests that $Ca(OH)_2$ treatment might be effectively used to improve strength of high carbonate composition materials and as a testing method to provide a more rapid determination of the self-cementation potential of silica-carbonate soils.
5. Scanning electron microscopic examinations of the soaked and tested materials showed that the observed strength gain variations were due to the different cement-particle bonding properties of carbonate cement–calcite particle and carbonate cement–quartz particle systems. Strength increases were more pronounced in high-carbonate materials because of good bonding of carbonate cement to calcite particles. In contrast, high-silica materials developed little or no strength increase because of a lack of bonding between carbonate cement and quartz particles.

ACKNOWLEDGMENT

The studies presented here were part of a project sponsored through a research grant from the Florida Department of Transportation (FDOT). The support and cooperation of the FDOT Bureau of Materials and Research is gratefully acknowledged.

REFERENCES

1. J. D. Gartland. *Florida Limerock Cementation Investigation*. Final Report. Department of Geology, University of Florida, Gainesville, Fla., 1979.

2. W. H. Zimpher. *Florida Limerock Investigation: Strength Gain Study of High and Low Carbonate Base Materials*. Final Report. Department of Civil Engineering, University of Florida, Gainesville, Fla., 1981.
3. R. E. Graves. *Strength Developed from Carbonate Cementation in Silica/Carbonate Systems*. Final Report. Department of Geology, University of Florida, Gainesville, Fla., 1987.
4. P. K. Weyl. The Solution Kinetics of Calcite. *Journal of Geology*, Vol. 66, 1958, pp. 163–176.
5. A. E. Z. Wissa and C. C. Ladd. *Shear Strength Generation in Stabilized Soils*. Research Report R65-17, Soils Publication No. 173. Department of Civil Engineering, Massachusetts Institute of Technology, Cambridge, Mass., June 1965.
6. S. K. Saxena and R. M. Lastrico. Static Properties of Lightly Cemented Sand. *Journal of the Geotechnical Engineering Division, ASCE*, Vol. 104, No. GT12, Dec. 1978, pp. 1449–1464.
7. *Florida Method of Test for Limerock Bearing Ratio, Designation: FM 5-515*. Florida Department of Transportation, Tallahassee, Fla., Sept. 1987.
8. J. P. Miller. A Portion of the System Calcium Carbonate–Carbon Dioxide–Water with Geological Implications. *American Journal of Science*, Vol. 250, 1952, pp. 161–203.
9. D. C. Thorstenson, F. T. Mackenzie, and B. L. Ristvet. Experimental Vadose and Phreatic Cementation of Skeletal Carbonate Sand. *Journal of Sedimentary Petrology*, Vol. 42, 1972, pp. 162–167.
10. E. C. Dapples. Diagenesis of Sandstones. In *Diagenesis in Sediments and Sedimentary Rocks*. (G. Larsen and G. V. Chilingar, eds.), Elsevier, Amsterdam, 1979.
11. G. W. Devore. Surface Chemistry as a Chemical Control on Mineral Association. *Journal of Geology*, Vol. 64, 1956, pp. 31–55.
12. R. G. C. Bathurst. *Carbonate Sediments and Their Diagenesis*, 2nd ed. Elsevier, Amsterdam, 1975.
13. R. S. Boynton. *Chemistry and Technology of Lime and Limestone*, 2nd ed. John Wiley and Sons, Inc., New York, 1980.
14. H. Blatt, G. Middleton, and R. Murray. *Origin of Sedimentary Rocks*. Prentice-Hall, Inc., Englewood Cliffs, N.J., 1980.